



Simulation of semiconductor devices

Internship report

Edmondo Valvo

Ingegneria Elettronica
Company Tutor : Gianluca Piccinini
Academic Tutor : Guido Masera

Index

1 Illuminated Semiconductor	3
1.1 Mesh	4
1.2 Regions	4
1.3 Electrodes	5
1.4 Doping	5
1.5 Materials	5
1.6 Models	5
1.7 Solve and Plot	5
1.8 Simulation Results	9
1.9 Theoretical analysis	11
1.10 Comparison with Shockley equation	13
1.11 Currents	15
1.12 Analysis for different lengths	21
1.13 $50 \mu_m$	21
1.14 $5\mu_m$	24
2 Haynes-Shockley experiment	26
2.1 Bias 0V	26
2.2 Bias 0,5V	29
2.3 Theoretical analysis	30
3 PN junction	34
3.1 Analysis	34
3.2 Band diagram, depletion region and electric field	34
3.3 Depletion region	37
3.4 Negative voltage	39
3.5 Positive voltage	42
3.6 Analysis of currents	43
3.7 Generation-Recombination effects	47
4 SRH recombination model	53
4.1 Fundamentals	53
4.2 Recombination rate	58
4.3 Padre comparison	59
4.4 Theoretical analysis	59
4.5 Simulation	60

The following report presents the curricular internship carried out during the third year of my bachelor's degree in Electronics engineering .

One of the most important goals of this experience has been to deepen the knowledge originally gained during the course "Electronic Devices" held by Professor Gianluca Piccinini, adviser of this project.

The main area of interest of this work is the simulation of various devices through an online tool called *Padre*, available on nanohub.org.

The analysis initially revolves around a simple piece of semiconductor with a light shining on its side and then a time-dependent observation of the same phenomenon which basically consists in the famous *Haynes-Shockley experiment*.

Chapter 3 contains the simulation of a *pn junction* from which an analysis of the *Shockley-Read-Hall recombination model (SRH)* became necessary in order to understand some recurring phenomena.

1 Illuminated Semiconductor

Let there be a uniformly p-doped semiconductor with impurity density $N_A=1e16$, a light source shining on its left side and various voltages applied at its extremities.

- p doping: $1 \cdot 10^{16} cm^{-3}$
- Semiconductor length: 1mm
- Generation: $2 \cdot 10^{22} cm^{-3} \cdot s^{-1}$ — low injection level
- Silicon, T=300K

In order to simulate this system an online tool called Padre, available on nanohub.org, was used. This platform through a specific coding language allows to simulate and analyze some interesting conditions for electronic devices. The code utilized in the experiment at hand is the following:

```
title      homogenous semiconductor (setup)
options    P0

mesh      rect nx=200 ny=4 outf=pdr520.mesh
x.m      n=1 l=0 r=1
x.m      n=40 l=0.01 r=1
x.m      n=200 l=1000 r=1
y.m      n=1 l=0 r=1
y.m      n=2 l=0.001 r=1
y.m      n=4 l=10 r=1

$ Regions specifications
region   num=1 ix.l=1 ix.h=40 iy.l=1 iy.h=4 silicon
region   num=2 ix.l=40 ix.h=200 iy.l=1 iy.h=4 silicon

elec num=1 ix.l=1 ix.h=1 iy.l=1 iy.h=4
elec num=2 ix.l=200 ix.h=200 iy.l=1 iy.h=4

$ Doping specification

dop    region=1 p.type conc=1e+16 uniform
dop    region=2 p.type conc=1e+16 uniform

plot.1d  log dop abs a.x=0 b.x=1000 b.y=10 a.y=10 points ascii
+          outf=pdr520.dop
```

```

$ Materials specifications
material name=silicon taun0=1e-06 taup0=1e-06

$ Specify models
models srh conmob fldmob temperature=300 print
system electrons holes newton

```

This first part physically describes the system under examination, it's useful to see the code as a series of blocks each describing a different characteristic .

1.1 Mesh

Firstly under “mesh” all the parameters on which the tool operates are defined:

- **rect:** indicates that it's a rectangular structure .
- **nx, ny:** The number of points, on each axis, that the software will utilize for the simulation .
- **x.m, y.m:** in these lines the actual physical dimensions of the system are defined, in fact there's a strict succession of parameters n, l and r. The parameter 'n' indicates on which point of the mesh, defined earlier, we're going to operate. 'l' is the value in μm of the point n, while 'r' indicates the resolution of that point in the simulation (just like the pixels in a screen) . The code above therefore represents a semiconductor with length 1mm, height 10 μm and , unless otherwise specified, the depth (z) is 1mm.

1.2 Regions

In this section the various regions of the semiconductor are defined. Regions are basically where the mesh points are grouped, they then get numbered and the material they consist of is also defined. Looking at the code it's clear that there are two regions:

- **The first** goes from 0 to 0.01 μm (from mesh point 1 to 40) on the x axis and from 0 to 10 μm on the y axis (from mesh point 1 to 4)
- **The second** occupies the remaining space. This division in two regions was made for convenience considering that the system at hand is a semiconductor illuminated on its side. In particular, during the actual simulation, the first region will be where all of the illumination takes place creating a very clear and easy to understand dicotomy.

1.3 Electrodes

The position of the two electrodes are defined following the same logic used with regions. It's extremely important to understand that **by omitting any other characteristic the contacts are assumed ohmic by Padre.**

1.4 Doping

As the name suggests here the doping profile is specified:

```
dop region=1 p.type conc=1e+16 uniform
```

- **Dop** indicates to Padre that the doping is about to be specified.
- We then have the region, the type, the concentration and the mode of doping, uniform in this case.

1.5 Materials

Under “Materials specifications” there is:

```
material name=silicon taun0=1e-06 taup0=1e-06
```

-material serves the exact same purpose dop did in the last command.

-taun and taup specify the electrons and holes' lifetimes .

Many more characteristics can be specified, such as energy gap or mobility for a given temperature .

1.6 Models

Here in the 'models' section the temperature and some physical models are specified, the latter are subsequently used by the tool for the various simulations.

1.7 Solve and Plot

In this second part of the code the actual simulations are carried out through the commands 'solve' and 'plot'. the code is the following:

```

$ Solve for initial conditions
solve init
plot.1d pot a.x=0 b.x=1000 a.y=10 b.y=10 ascii outf=pdr520.pot SP
plot.1d band.val a.x=0 b.x=1000 a.y=10 b.y=10 ascii outf=pdr520.vband
plot.1d band.con a.x=0 b.x=1000 a.y=10 b.y=10 ascii outf=pdr520.cband
plot.1d qfn a.x=0 b.x=1000 a.y=10 b.y=10 ascii outf=pdr520.qfn
plot.1d qfp a.x=0 b.x=1000 a.y=10 b.y=10 ascii outf=pdr520.qfp
plot.1d ele a.x=0 b.x=1000 a.y=10 b.y=10 ascii outf=pdr520.ele
plot.1d hole a.x=0 b.x=1000 a.y=10 b.y=10 ascii outf=pdr520.hole
plot.1d net.charge a.x=0 b.x=1000 a.y=10 b.y=10 ascii outf=pdr520.ro
plot.1d e.field a.x=0 b.x=1000 a.y=10 b.y=10 ascii outf=pdr520.efield
plot.1d recomb a.x=0 b.x=1000 a.y=10 b.y=10 ascii outf=pdr520.recomb +
+ SPLINE NSPLINE=200

solve gen=2.001e22 reg.gen=1 absorp=0 dir.gen=x
plot.1d pot a.x=0 b.x=1000 a.y=10 b.y=10 ascii outf=pdr520.pot SP
plot.1d band.val a.x=0 b.x=1000 a.y=10 b.y=10 ascii outf=pdr520.vband
plot.1d band.con a.x=0 b.x=1000 a.y=10 b.y=10 ascii outf=pdr520.cband
plot.1d qfn a.x=0 b.x=1000 a.y=10 b.y=10 ascii outf=pdr520.qfn
plot.1d qfp a.x=0 b.x=1000 a.y=10 b.y=10 ascii outf=pdr520.qfp
plot.1d ele a.x=0 b.x=1000 a.y=10 b.y=10 ascii outf=pdr520.ele
plot.1d hole a.x=0 b.x=1000 a.y=10 b.y=10 ascii outf=pdr520.hole
plot.1d net.charge a.x=0 b.x=1000 a.y=10 b.y=10 ascii outf=pdr520.ro
plot.1d e.field a.x=0 b.x=1000 a.y=10 b.y=10 ascii outf=pdr520.efield
plot.1d recomb a.x=0 b.x=1000 a.y=10 b.y=10 ascii outf=pdr520.recomb +
+ SPLINE NSPLINE=200
plot.1d j.electron a.x=0 b.x=1000 a.y=10 b.y=10 ascii outf=pdr520.jelectron
plot.1d j.hole a.x=0 b.x=1000 a.y=10 b.y=10 ascii outf=pdr520.jhole
plot.1d j.total a.x=0 b.x=1000 a.y=10 b.y=10 ascii outf=pdr520.jtot

solve v1=1.5 elect=1
solve gen=2e22 reg.gen=1 absorp=0 dir.gen=x
plot.1d pot a.x=0 b.x=1000 a.y=10 b.y=10 ascii outf=pdr520.pot SP
plot.1d band.val a.x=0 b.x=1000 a.y=10 b.y=10 ascii outf=pdr520.vband
plot.1d band.con a.x=0 b.x=1000 a.y=10 b.y=10 ascii outf=pdr520.cband
plot.1d qfn a.x=0 b.x=1000 a.y=10 b.y=10 ascii outf=pdr520.qfn
plot.1d qfp a.x=0 b.x=1000 a.y=10 b.y=10 ascii outf=pdr520.qfp
plot.1d ele a.x=0 b.x=1000 a.y=10 b.y=10 ascii outf=pdr520.ele
plot.1d hole a.x=0 b.x=1000 a.y=10 b.y=10 ascii outf=pdr520.hole
plot.1d net.charge a.x=0 b.x=1000 a.y=10 b.y=10 ascii outf=pdr520.ro
plot.1d e.field a.x=0 b.x=1000 a.y=10 b.y=10 ascii outf=pdr520.efield

```

```

plot.1d recomb a.x=0 b.x=1000 a.y=10 b.y=10 ascii outf=pdr520.recomb+
+ SPLINE NSPLINE=200
plot.1d j.electron a.x=0 b.x=1000 a.y=10 b.y=10 ascii outf=pdr520.jelectron
plot.1d j.hole a.x=0 b.x=1000 a.y=10 b.y=10 ascii outf=pdr520.jhole
plot.1d j.total a.x=0 b.x=1000 a.y=10 b.y=10 ascii outf=pdr520.jtot

```

At first the system is simulated at equilibrium, without any voltage applied to it or generation of carriers. This is easily achieved through:

solve init

After the 'solve line' some parameters are plotted in order to visualize them, for example:

```

plot.1d band.val a.x=0 b.x=1000 a.y=10 b.y=10 ascii
outf=pdr520.vband

```

The behavior of the valence band in the region $x \in [0,1]\text{mm}$ and $y \in [0,10]\mu\text{m}$ will be shown, basically the whole semiconductor.

Subsequently the light source is added on the left side of the system:

solve gen=2.001e22 reg.gen=1 absorp=0 dir.gen=x

- **gen** is the generation term expressed in units/($s \cdot cm^3$).
- **reg.gen** specifies the region in which the generation takes place, this is why it was originally chosen to create two separate zones: one that represents the majority of the semiconductor, the other (much smaller) in which the generation happens.
- **absorp** (absorption) establishes an absorption coefficient for the radiation ($1/\mu m$).
- **dir.gen** points out the axis along which the radiation penetrates.

Following this there are a few solve lines that simulate some other bias points:

solve v1=1.5 elect=1
solve gen=2e22 reg.gen=1 absorp=0 dir.gen=x

The specifics of the radiation are maintained but a different voltage is applied on electrode 1 (1.5V).

In some situations it's crucial to have a very precise order in the execution of the solve lines. This is due to the fact that Padre bases each simulation on predictions derived from the previous simulations, this is precisely why there's often a 'solve init' line before anything else. Sometimes failing to follow this methodology will lead to convergence errors .

The keyword end is used to point out the end of the file :

```
plot.1d j.electron a.x=0 b.x=1000 a.y=10 b.y=10 ascii outf=pdr520.jelectron  
plot.1d j.hole a.x=0 b.x=1000 a.y=10 b.y=10 ascii outf=pdr520.jhole  
plot.1d j.total a.x=0 b.x=1000 a.y=10 b.y=10 ascii outf=pdr520.jtot  
  
end
```

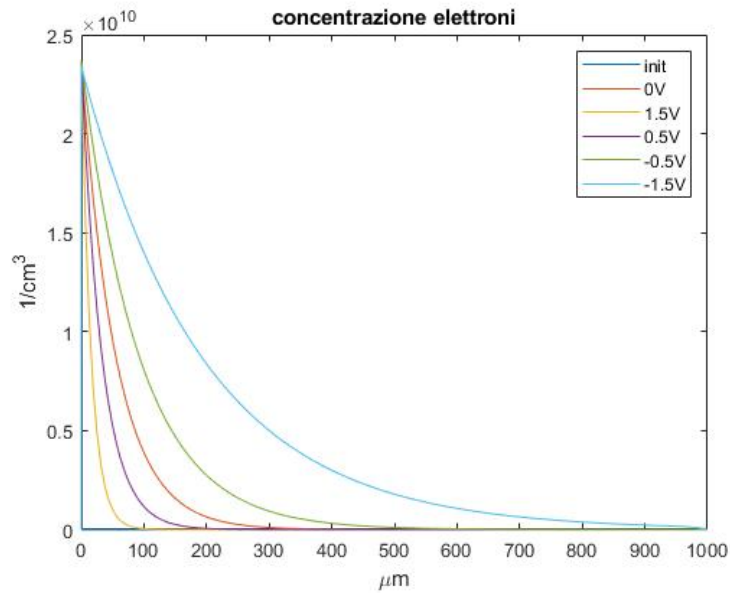


Figure 1: Concentration of electrons (simulation)

1.8 Simulation Results

The results of the simulations can be exported after running the code, this allows us to analyze them on Matlab making the whole process easier.

For the system in question the results are shown in the figures 1,2 and 3.

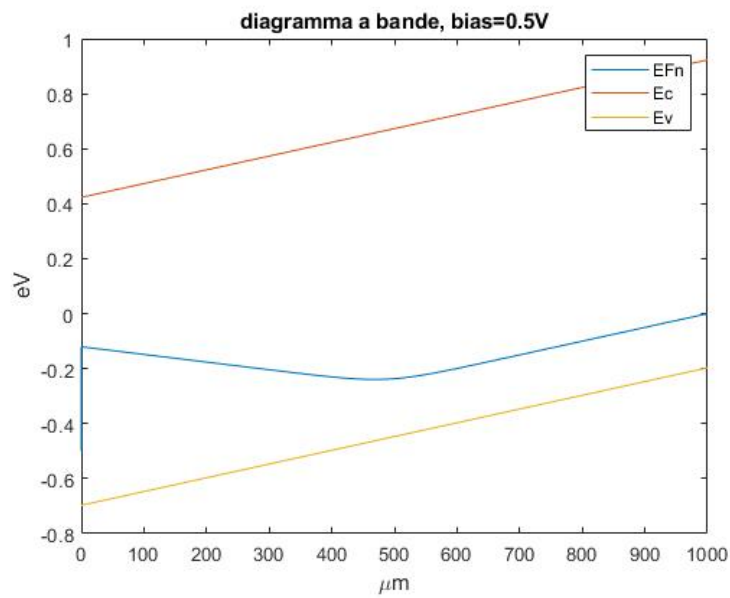


Figure 2: band diagram bias=0,5V

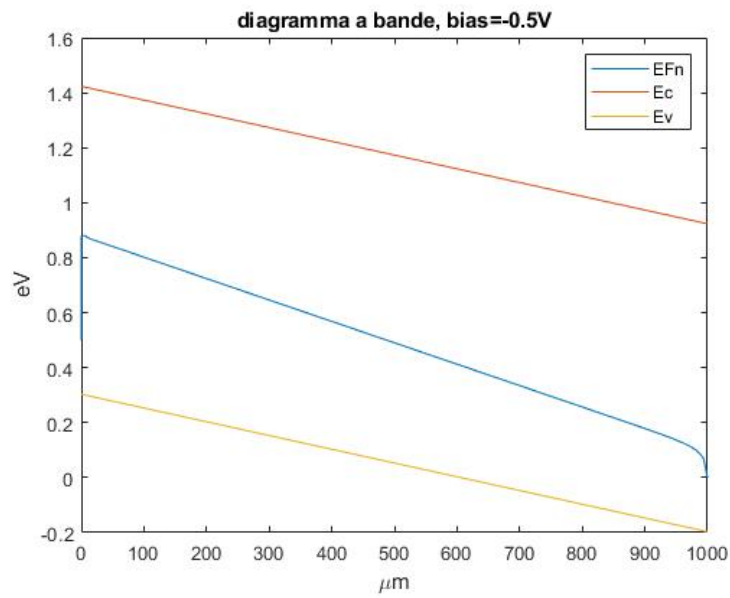
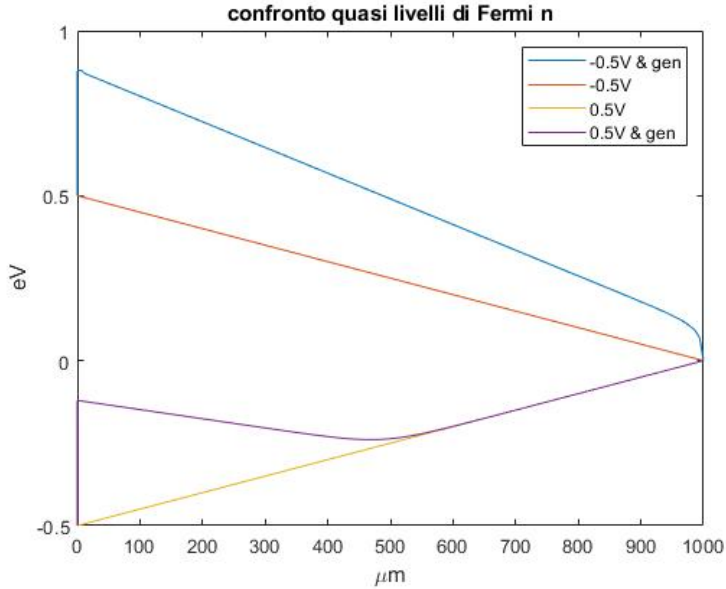


Figure 3: band diagram, bias=-0,5V



Something interesting is going on on the left side of the semiconductor, which is where illumination and voltage application take place.

Intuitively, it's easy to imagine that the excess carriers, greatly increasing the overall electron concentration, initially make the Fermi level rise towards the conduction band and then, as the electrons recombine, it will go back to its equilibrium state.

This behavior will change depending on the applied bias:

- **For negative voltages** there's an electric field that makes the electrons move in the positive direction of the x axis.
- **For positive voltages** the electric field 'tries to keep' the electrons close to the left side of the semiconductor, this is why the concentration level of electrons goes back to its equilibrium value faster in this case.

1.9 Theoretical analysis

It's now appropriate to analyze the situation from a theoretical standpoint. From the drift-diffusion equation:

$$J_n = qn\mu_n\varepsilon + qD_n \frac{dn}{dx} \quad (1)$$

Replacing the appropriate value in the continuity equation and imposing the stationarity ($\frac{dn}{dt} = 0$) we get :

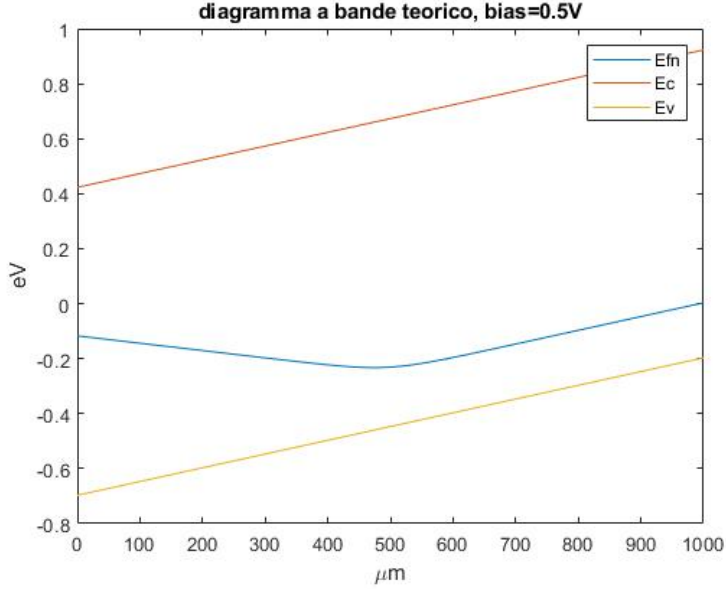


Figure 4: band diagram obtained from calculation

$$\frac{(d^2n')}{(dx^2)} + \frac{(V_a)}{(LV_t)} \frac{dn'}{dx} - \frac{n'}{\tau_n} = 0 \quad (2)$$

Where n' are the excess electrons and V_a is the applied bias .

The solution of the differential equation gives:
for bias=0,5V

$$n' = n'(0)e^{-0,02965x} = 2.36e10 \cdot e^{-0,02965x} \quad (3)$$

for bias=-0,5V

$$n' = n'(0)e^{-0,02965x} = 2.36e10 \cdot e^{-0,01041x} \quad (4)$$

(The coefficient in the differential equation solution is expressed in μm since the points on the x axis are given in μm by the simulation). Using this expression it's possible to get the quasi-Fermi level :

$$E_{fn} = E_c + KT \cdot \ln\left(\frac{n_0 + n'}{N_c}\right) \quad (5)$$

We can get the band diagram with the 'theoretical' value of the quasi-Fermi level by plugging this relation in Matlab and using as E_c and n_0 the values given by the simulation.

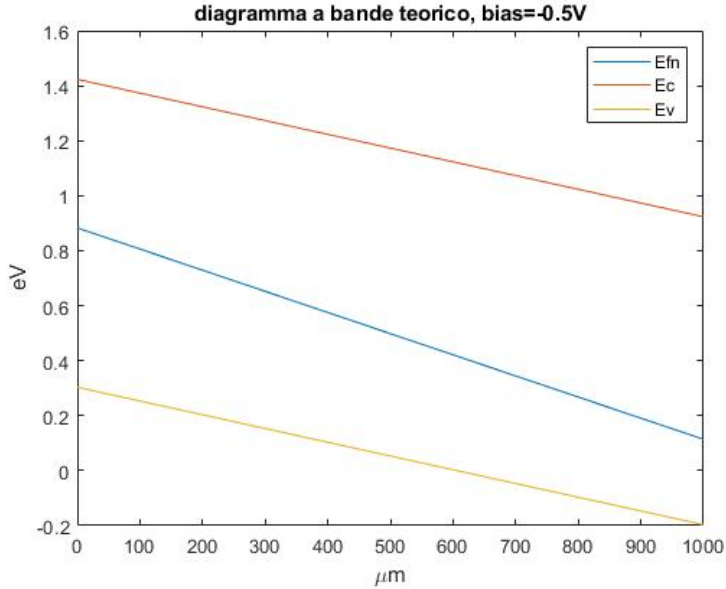


Figure 5: band diagram obtained from calculation

There's a very close correspondence between simulation and theoretical prediction.

1.10 Comparison with Shockley equation

Up until now two elements have been analyzed: quasi-Fermi level and electron concentration. The Shockley equation binds these two values together through:

$$n = n_i \cdot e^{\frac{E_f - E_i}{KT}} \quad (6)$$

To check how this equation holds in practice we swap the variables with the values obtained from the simulation.

It's immediately clear that there's a strong resemblance between figures 1 and 6.

To check this relation further the comparison between the simulation and Shockley electron concentrations is shown in figures 7 and 8 in the two bias points 0,5V and -0,5V.

The difference in the curves is due to a difference in the initial value, getting it perfectly would result in a quasi-perfect match of the two curves.

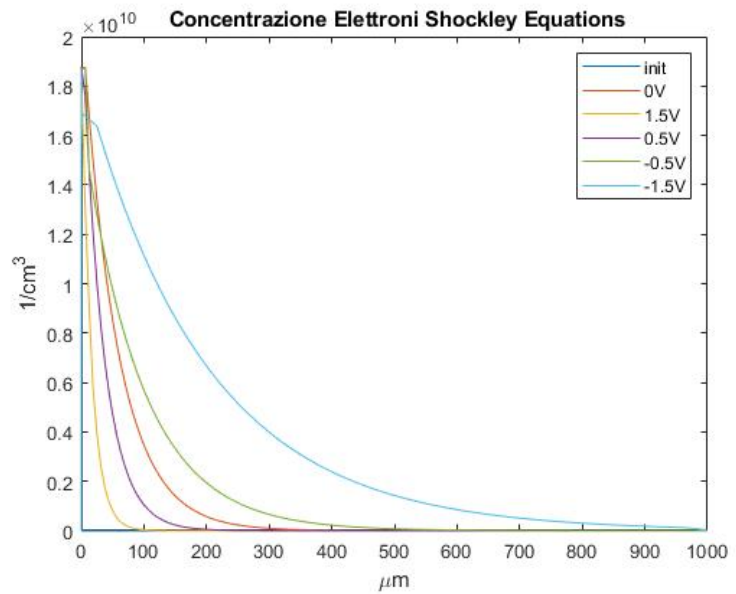


Figure 6: Electron concentration modeled by Shockley equation

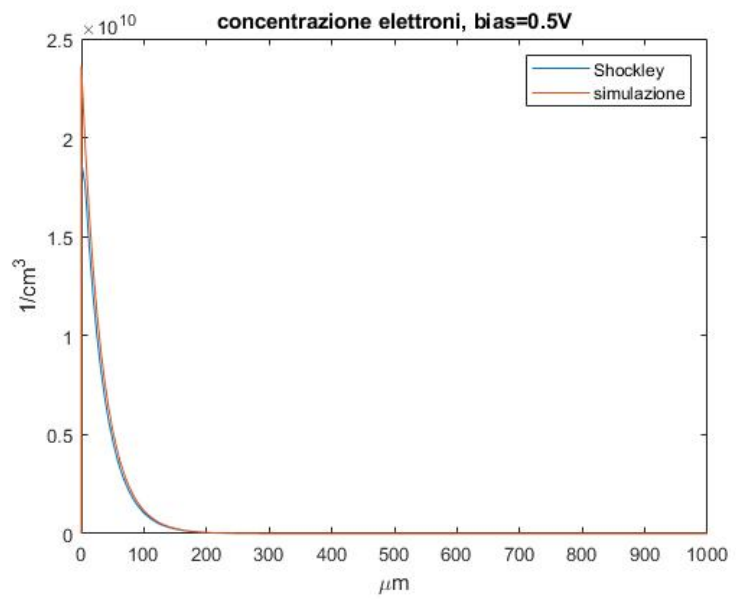


Figure 7: Shockley (blue) e Padre(red)

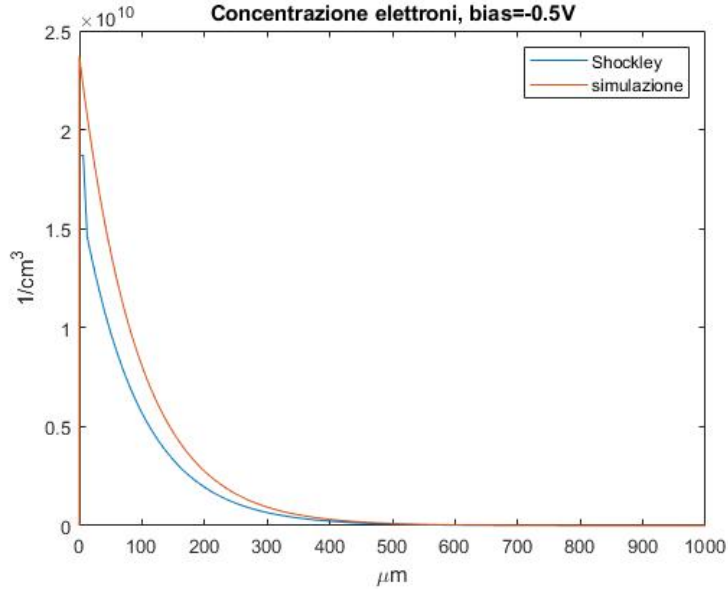


Figure 8: Shockley (blue) e Padre(red)

1.11 Currents

The currents in the illuminated semiconductor are:

$$J_n = qn\mu_n\varepsilon + qD_n \frac{dn}{dx} = qn_{p0}\mu_n \frac{V_a}{L} + qn'\mu_n \frac{V_a}{L} + qD_n \frac{dn}{dx} \quad (7)$$

For n' are used the expressions previously obtained .

The results are shown in figures 9 and 10.

There's again a very close match between calculations and simulation. However a closer inspection reveals some inconsistencies between 0 and $6.26\mu_m$ in both cases.

Given this strong difference it's important to look for some theoretical assumption that ,if not verified, might lead to the departure in the graphs.

An assumption originally made but never actually verified was that of quasi neutrality, it was in fact assumed that the electric field was simply $\frac{V_a}{L}$ which is wrong if there's a substantial charge distribution unaccounted for.

The net charge is:

$$\rho = q(p - n + Na - Nd) \quad (8)$$

Which, in our case, simplifies to:

$$\rho = q(p' - n' - n) \quad (9)$$

(p' was obtained through the same process used for n')

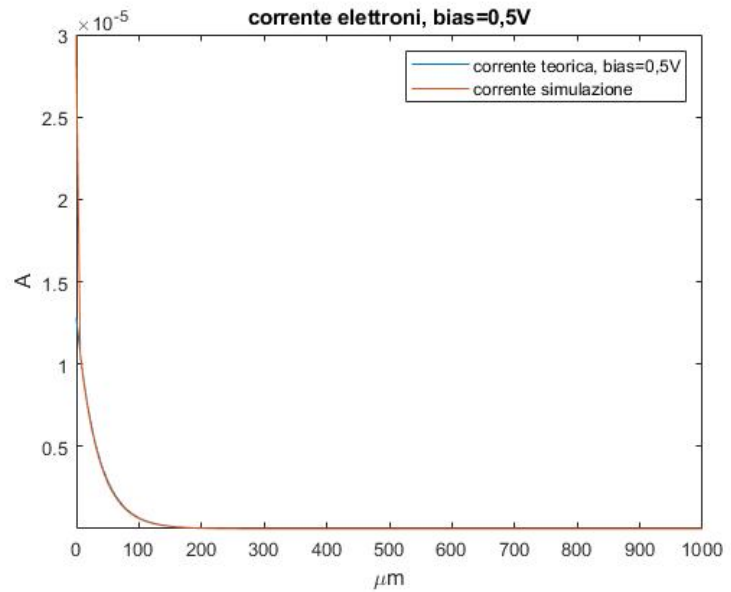


Figure 9: currents comparison, bias=0,5V

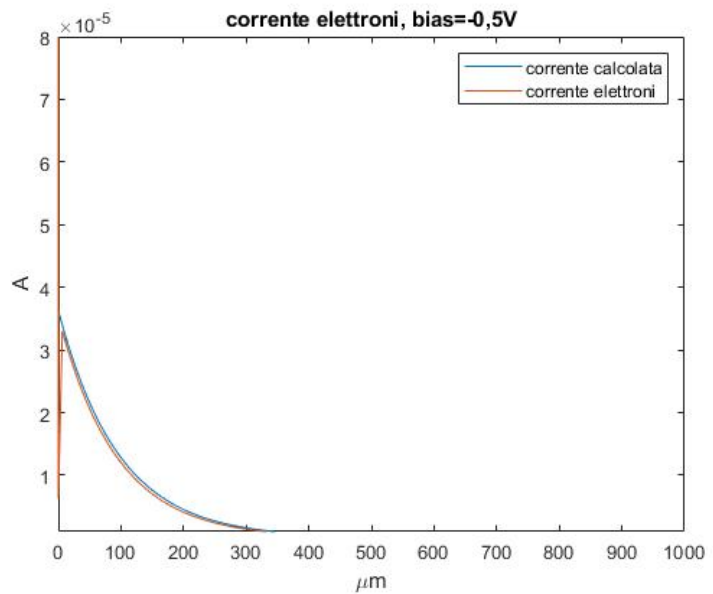


Figure 10: currents comparison,bias=-0,5V

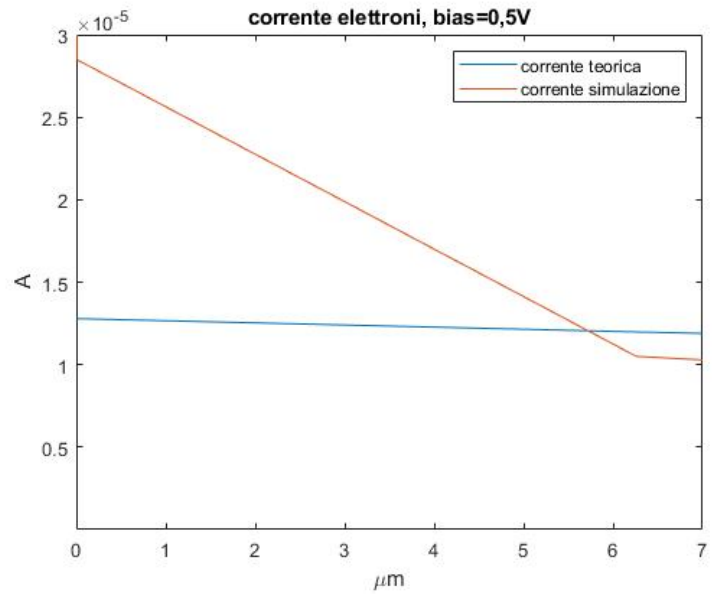


Figure 11: Current for bias=0,5V between 0 and 7 μm

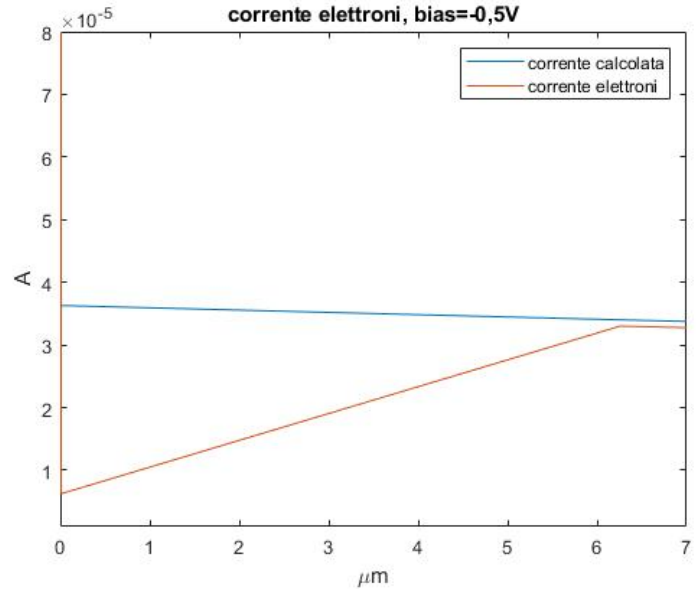


Figure 12: Current for bias=-0,5V between 0 and 7 μm

for bias=0,5V:

$$p' = p'(0)e^{-0,02264x} = 2.2410^{10}e^{-0,02264x} \quad (10)$$

for bias=-0,5V:

$$p' = p'(0)e^{-0,04188x} = 2.2410^{10}e^{-0,04188x} \quad (11)$$

Plotting this expression and comparing it with the simulation gives figures 13 and 14.

These results can once again be interpreted intuitively. For positive bias the electric field keeps the electrons close to the left side of the semiconductor facilitating the recombination process

Even though the values are of the order of $e-9$ there's still a big difference between the two cases , in fact the simulation value goes very quickly to 0 before $6.26\mu_m$.

A fundamental difference between simulation and theory is the recombination model, in Padre the Shockley-Read-Hall model was used while in the theoretical calcualtions we used the simpler direct recombination model.

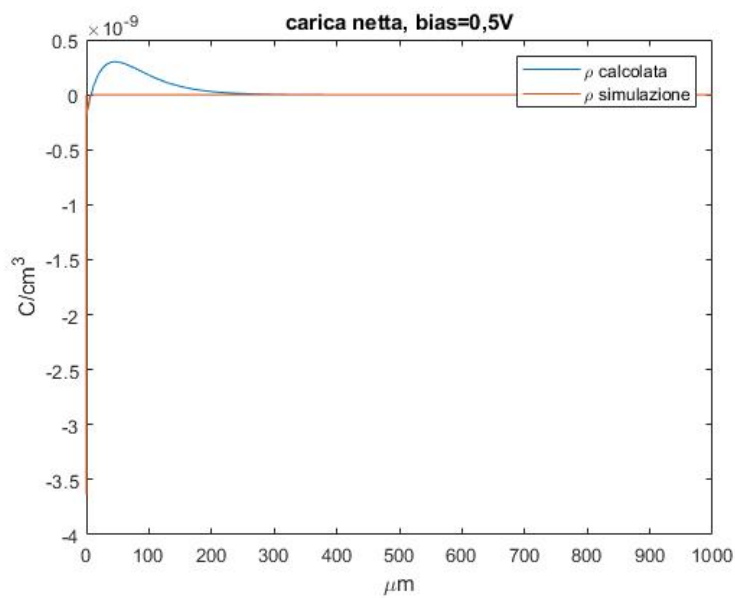


Figure 13: Net charge comparison for bias=0,5V

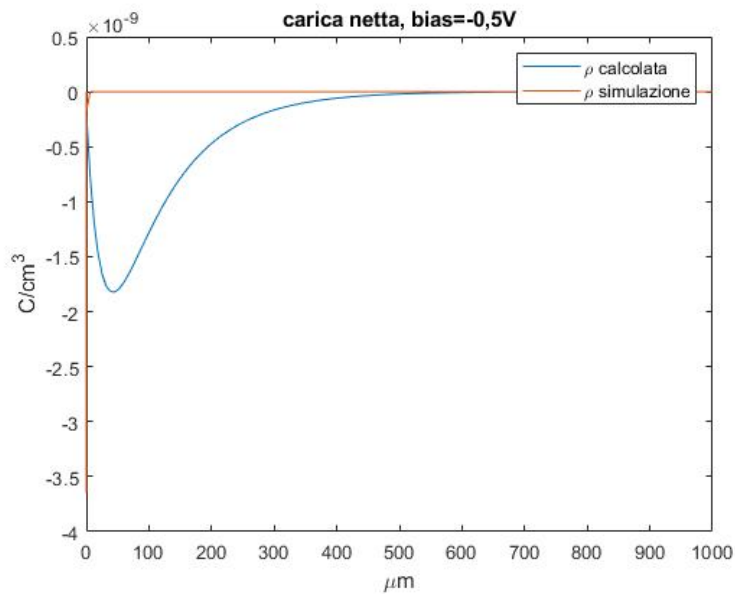


Figure 14: Net charge comparison for bias=-0,5V

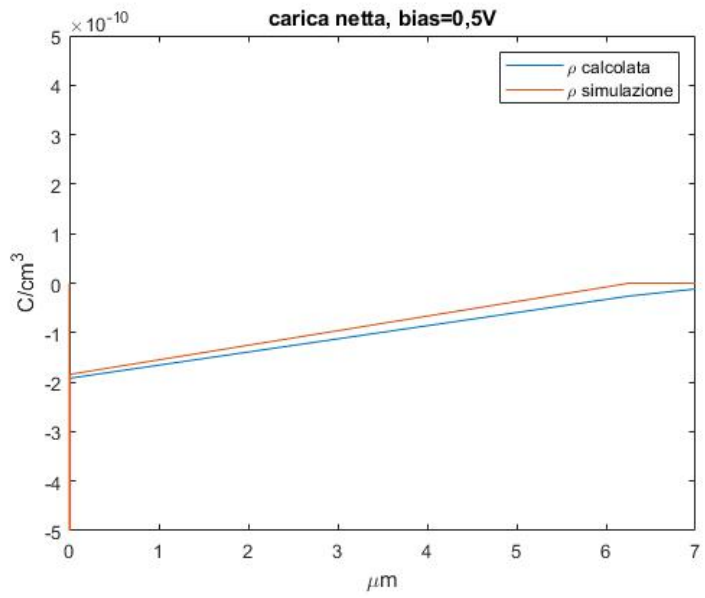


Figure 15: Net charge comparison between 0 and $7\mu_m$ for bias=0,5V

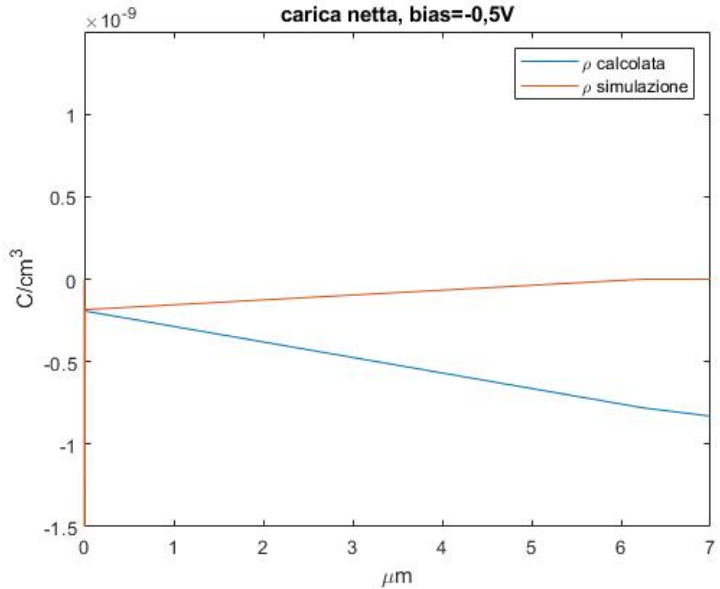


Figure 16: Net charge comparison between 0 and $7\mu_m$ for bias=-0,5V

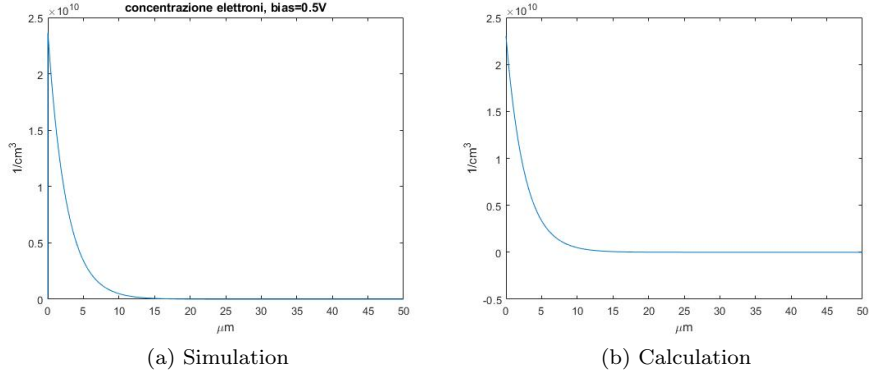


Figure 17: concentrations for bias=0.5V

1.12 Analysis for different lengths

The same analysis done previously can be repeated for various lengths, such as $5\mu_m$ and $50\mu_m$.

1.13 $50 \mu_m$

Following the same steps as before we get the expressions for minority carriers :
-for bias $V_a=0,5V$

$$n' = -101.4 \cdot e^{0.00081137x} + 2.3 \cdot 10^{10} \cdot e^{-0.38541x} \quad (12)$$

-for bias $V_a=-0,5V$

$$n' = -94.4 \cdot e^{0.38541x} + 2.3 \cdot 10^{10} \cdot e^{-0.00081x} \quad (13)$$

In figures 17 and 18 a comparison between these expressions and the simulation results is shown.

Figure 19 and 20 show the same comparison but for quasi-Fermi levels .

Just like the previous case, figures 21 and 22 show a good resemblance in the comparison with the Shockley equations albeit with a difference caused by the initial value.

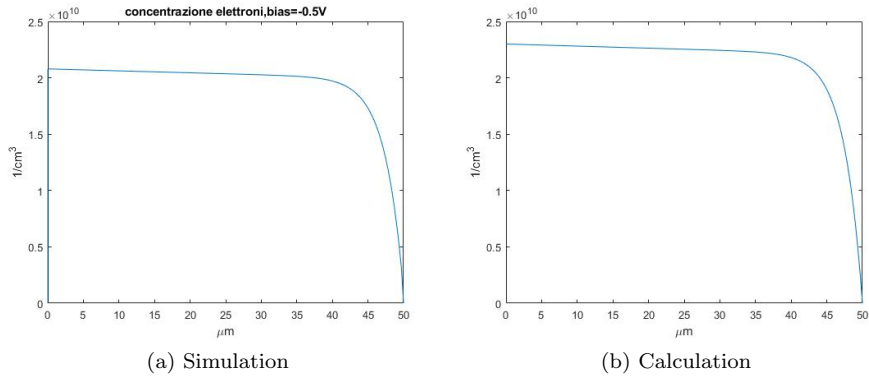


Figure 18: Concentrations for bias=-0.5V

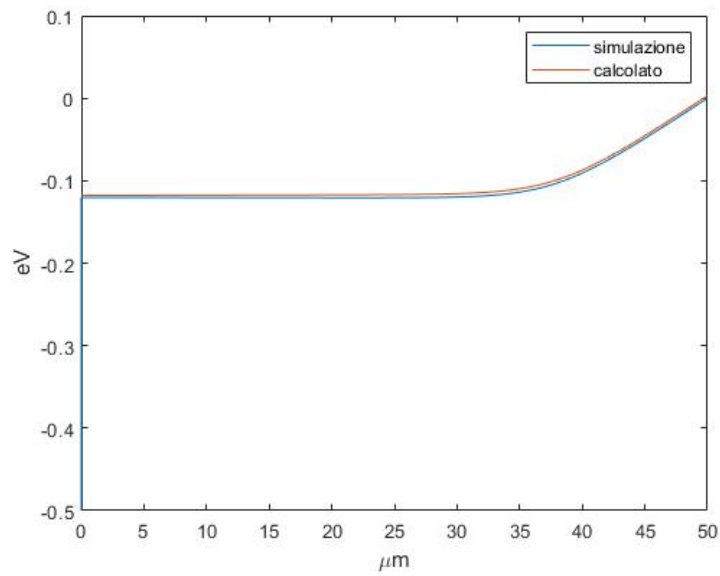


Figure 19: Comparison of Quasi-Fermi levels for bias=0,5V

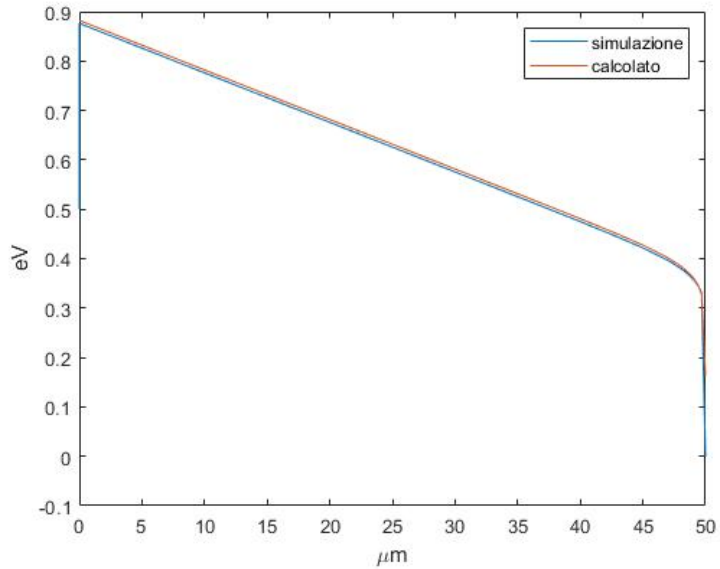


Figure 20: Comparison of Quasi-Fermi levels for bias=-0,5V

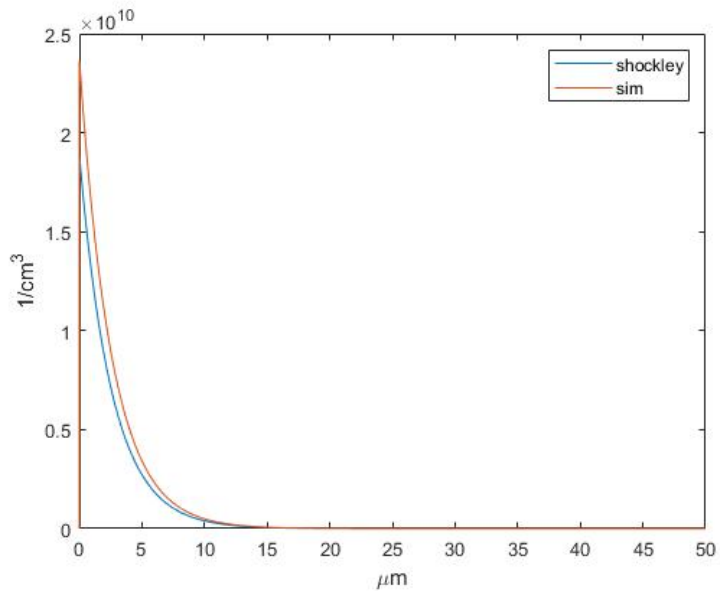


Figure 21: Comparison with Shockley for bias=0,5V

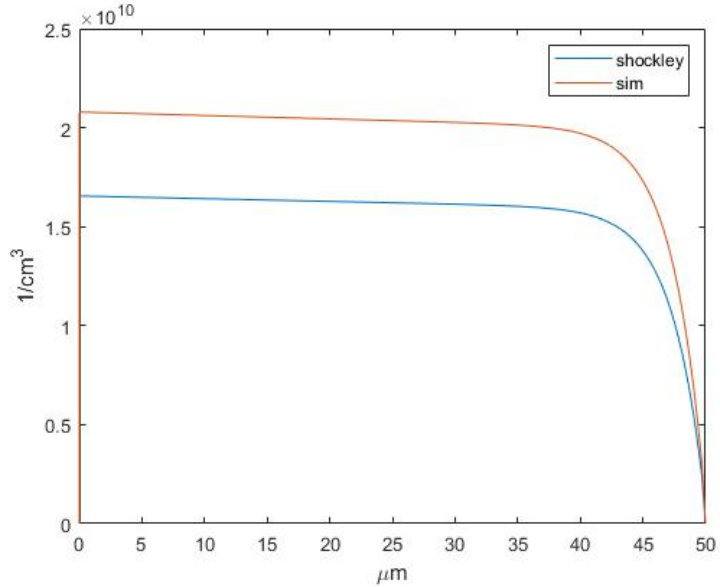


Figure 22: Comparison with Shockley for bias=-0,5V

1.14 $5\mu_m$

Following the same procedure we get:

-for bias=0,5V

$$n' = -102.3 \cdot e^{0.000150766x} + 2.3 \cdot 10^{10} \cdot e^{-3.846x} \quad (14)$$

-for bias=-0,5V

$$n' = -42.93 \cdot e^{3.846x} + 9.651 \cdot 10^9 \cdot e^{-0.000150766x} \quad (15)$$

The only real difference between theory and simulation is in the case with applied bias -0.5V. Padre keeps the contacts neutral by putting the carriers concentrations to 0 but still shows a good amount of charges accumulated on the left side of the semiconductor which isn't accurately described by the, overly simplified, theoretical model.

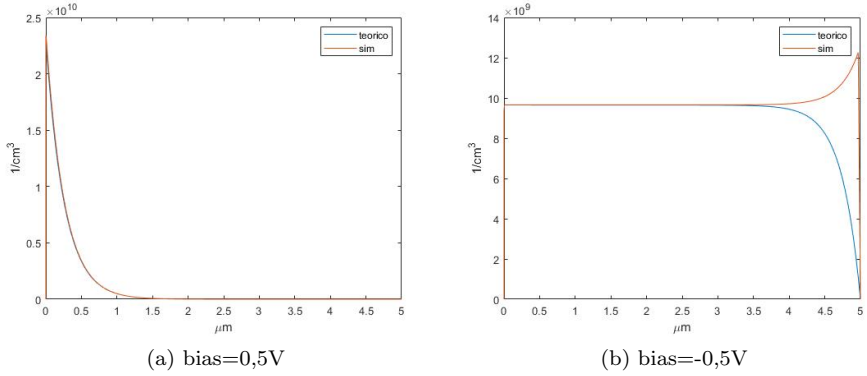


Figure 23: Comparison of electron concentrations

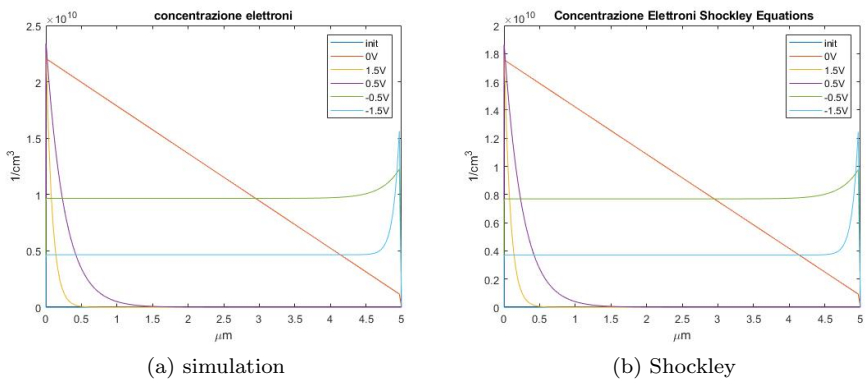


Figure 24: Shockley and simulation comparison

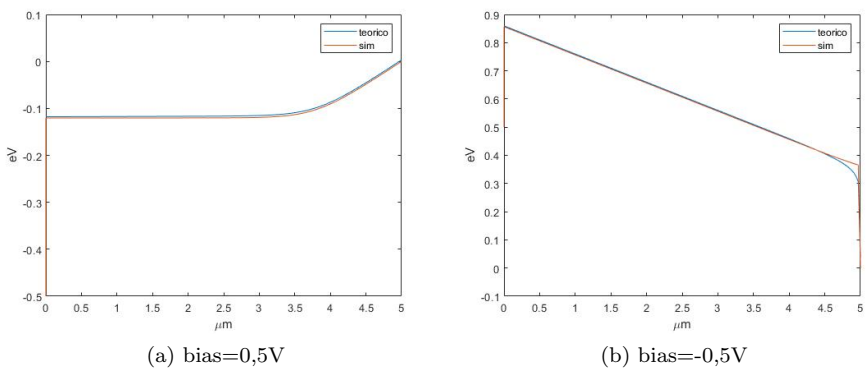


Figure 25: Quasi-Fermi levels comparison

2 Haynes-Shockley experiment

Padre also makes it possible to analyze the time evolution of semiconductor devices which becomes crucial in cases like the Haynes-Shockley experiment.

This classical experiment consists of generating some excess carriers and analyzing the subsequent diffusion processes.

Two situations were simulated, one with bias=0V and the other one with bias=0.5V.

2.1 Bias 0V

We have a 2mm semiconductor slab with height 10 μm and uniform p-doping 10^{16} cm^{-3}

Besides the physical dimension the characteristics are exactly the same as before with the illuminated semiconductor.

Region 2 is defined so that all the generation takes place there and it becomes easier to code the solve lines.

After having simulated the system at equilibrium we move on to the illumination by inserting a uniform radiation in the space between $x = 1000\mu_m$ a $x = 1001\mu_m$.

In the second solve line there's the very first time dependent analysis with a generation that has a rise time $g.\tau$ equal to 5e-15s, which basically means that it reaches its peak at $t=5\text{e-15s}$, and then stops at $t=1\text{ps}$. The following line of code specifies that the generation falls off with a fall time of 5ps and the whole simulation will stop at $t=21\text{ps}$.

This process is repeated for different time intervals in figures 28 and 29.

It's clear from the graphs that, as time goes on, the carriers, through the process of diffusion, go back to their equilibrium value.

This simulation produces the results shown in figure 30.

```

|title      homogenous semiconductor (setup)
|options    P0

mesh      rect nx=200 ny=4 outf=pdr826.mesh
x.m      n=1 l=0 r=1.01
x.m      n=40 l=1000 r=0.99
x.m      n=80 l=1000.001 r=1.01
x.m      n=120 l=1001 r=0.99
x.m      n=200 l=2000 r=1.01
y.m      n=1 l=0 r=1
y.m      n=2 l=0.001 r=1
y.m      n=4 l=10 r=1

$ Regions specifications
region   num=1 ix.l=1 ix.h=40 iy.l=1 iy.h=4 silicon
region   num=2 ix.l=40 ix.h=120 iy.l=1 iy.h=4 silicon
region   num=3 ix.l=120 ix.h=200 iy.l=1 iy.h=4 silicon

elec num=1 ix.l=1 ix.h=1 iy.l=1 iy.h=4
elec num=2 ix.l=200 ix.h=200 iy.l=1 iy.h=4

$ Doping specification
dop   region=1 p.type conc=1e+16 uniform
dop   region=2 p.type conc=1e+16 uniform
dop   region=3 p.type conc=1e+16 uniform
plot.1d log dop abs a.x=0 b.x= 500 b.y=10 a.y=10 points ascii
+          outf=pdr826.dop

$ Materials specifications
material name=silicon taun0=1e-06 taup0=1e-06

$ Specify models
models srh conmob fldmob temperature=300 print
system electrons holes newton

```

Figure 26: Padre code

```

$ Solve for initial conditions
solve init
plot.1d pot a.x=0 b.x=2000 a.y=10 b.y=10 ascii outf=pdr826.pot SP
plot.1d band.val a.x=0 b.x=2000 a.y=10 b.y=10 ascii outf=pdr826.vband
plot.1d band.con a.x=0 b.x=2000 a.y=10 b.y=10 ascii outf=pdr826.cband
plot.1d qfn a.x=0 b.x=2000 a.y=10 b.y=10 ascii outf=pdr826.qfn
plot.1d qfp a.x=0 b.x=2000 a.y=10 b.y=10 ascii outf=pdr826.qfp
plot.1d ele a.x=0 b.x=2000 a.y=10 b.y=10 ascii outf=pdr826.ele
plot.1d hole a.x=0 b.x=2000 a.y=10 b.y=10 ascii outf=pdr826.hole
plot.1d net.charge a.x=0 b.x=2000 a.y=10 b.y=10 ascii outf=pdr826.ro
plot.1d e.field a.x=0 b.x=2000 a.y=10 b.y=10 ascii outf=pdr826.efield
plot.1d recomb a.x=0 b.x=2000 a.y=10 b.y=10 ascii outf=pdr826.recomb SPLINE NSPLINE=200

$ Solve for light source
log outf=gen0
solve GEN=2e22 REG.GEN=2 ABSORP=0 DIR.GEN=y
+ G.TAU=5e-15 TSTEP=1e-10 TSTOP=1e-12
solve G.TAU=5e-12 TSTOP=2.1e-11
plot.1d pot a.x=0 b.x=2000 a.y=10 b.y=10 ascii outf=pdr826.pot SP
plot.1d band.val a.x=0 b.x=2000 a.y=10 b.y=10 ascii outf=pdr826.vband
plot.1d band.con a.x=0 b.x=2000 a.y=10 b.y=10 ascii outf=pdr826.cband
plot.1d qfn a.x=0 b.x=2000 a.y=10 b.y=10 ascii outf=pdr826.qfn
plot.1d qfp a.x=0 b.x=2000 a.y=10 b.y=10 ascii outf=pdr826.qfp
plot.1d ele a.x=0 b.x=2000 a.y=10 b.y=10 ascii outf=pdr826.ele
plot.1d hole a.x=0 b.x=2000 a.y=10 b.y=10 ascii outf=pdr826.hole
plot.1d net.charge a.x=0 b.x=2000 a.y=10 b.y=10 ascii outf=pdr826.ro
plot.1d e.field a.x=0 b.x=2000 a.y=10 b.y=10 ascii outf=pdr826.efield
plot.1d recomb a.x=0 b.x=2000 a.y=10 b.y=10 ascii outf=pdr826.recomb SPLINE NSPLINE=200

```

Figure 27: first two solve lines (initial conditions and illumination)

<pre> solve init solve GEN=2e22 REG.GEN=2 ABSORP=0 DIR.GEN=y + G.TAU=5e-15 TSTEP=1e-10 TSTOP=1e-12 solve G.TAU=5e-12 TSTOP=3.1e-11 </pre>	<pre> solve init solve GEN=2e22 REG.GEN=2 ABSORP=0 DIR.GEN=y + G.TAU=5e-15 TSTEP=1e-10 TSTOP=1e-12 solve G.TAU=5e-12 TSTOP=1.1e-8 </pre>
---	--

(a) t=31ps

(b) t=11ns

Figure 28: Solve lines for various time values

<pre> solve init solve GEN=2e22 REG.GEN=2 ABSORP=0 DIR.GEN=y + G.TAU=5e-15 TSTEP=1e-10 TSTOP=1e-12 solve G.TAU=5e-12 TSTOP=7e-7 </pre>	<pre> solve init solve GEN=2e22 REG.GEN=2 ABSORP=0 DIR.GEN=y + G.TAU=5e-15 TSTEP=1e-10 TSTOP=1e-12 solve G.TAU=5e-12 TSTOP=1.1e-5 </pre>
--	--

(a) t=0, 7

(b) t=11

Figure 29: Solve lines for various time values

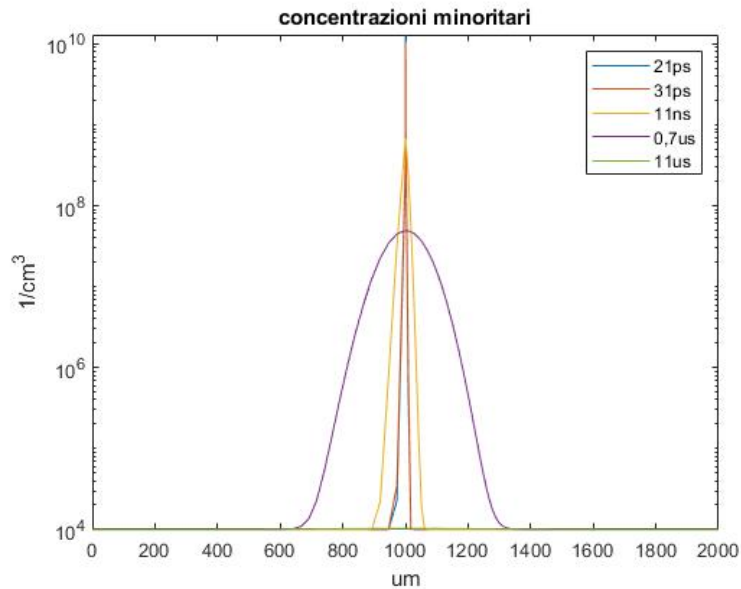


Figure 30: Electron concentration simulated for different time instants

```

solve v1=0.5
solve GEN=2e22 REG.GEN=2 ABSORP=0 DIR.GEN=y
+ G.TAU=5e-15 TSTEP=1e-10 TSTOP=1e-12
solve G.TAU=5e-12 TSTOP=3.1e-11

```

Figure 31: Addition of bias to the Solve line

2.2 Bias 0,5V

In this case besides diffusion there's also a drift component caused by the electric field.

The only change made to the code consists in the addition of the following:

solve v1=0.5

Leading to the code shown in figure 31 and the distribution of figure 32.

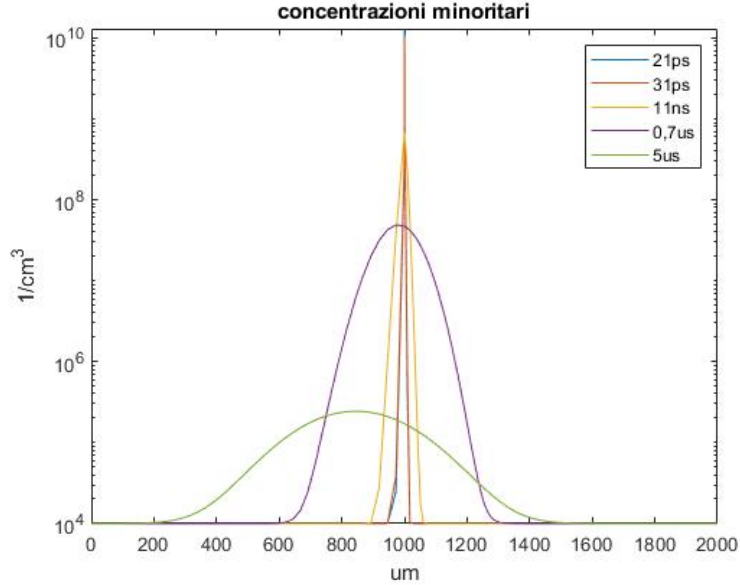


Figure 32: Electron concentration simulated in various time intervals

2.3 Theoretical analysis

The Drift-Diffusion equations give us:

$$\frac{dn'}{dt} - \mu_n \varepsilon \frac{dn'}{dx} - D_n \frac{d^2 n'}{dx^2} + \frac{n'}{\tau_n} = 0 \quad (16)$$

In this case the solution must be of the following form:

$$n' = \frac{H}{\sqrt{Bt}} \cdot e^{-\frac{(x-vt)^2}{Ct} - \frac{t}{E}} \quad (17)$$

With H,B,v,C and E parameters to be found.

It's now possible to calculate $\frac{dn'}{dt}$, $\frac{dn'}{dx}$, $\frac{d^2 n'}{dx^2}$ and insert them in (16):

$$\frac{H}{\sqrt{Bt}} \cdot e^\eta \cdot \left[\frac{-1}{2t} + \frac{x-vt}{Ct} (2v + 2\mu_n \varepsilon) + \frac{(x-vt)^2}{(Ct)^2} (C - 4D_n) - \frac{1}{E} + \frac{2D_n}{Ct} \right] = \frac{-n'}{\tau_n} \quad (18)$$

with $\eta = -\frac{(x-vt)^2}{Ct} - \frac{t}{E}$.

By comparison with equation (17) it's immediately clear that $v = -\mu_n \varepsilon$ and $C = 4D_n$, which yield:

$$\frac{H}{\sqrt{Bt}} \cdot e^\eta \cdot \left[-\frac{1}{2t} - \frac{1}{E} + \frac{1}{2t} \right] = -\frac{H}{\sqrt{Bt}} \cdot e^\eta \cdot \frac{1}{E} = -\frac{n'}{\tau_n} \quad (19)$$

Comparing again with (17) we put $E = \tau_n$, obtaining the following:

$$n' = \frac{H}{\sqrt{Bt}} e^\eta \quad (20)$$

The parameters H and B still have to be determined, to do so we calculate the number of electrons generated at t=0 with electric field equal to zero.

$$N = A \int_{-\infty}^{+\infty} \frac{H}{\sqrt{Bt}} e^\eta dx = A \int_{-\infty}^{+\infty} \frac{H}{\sqrt{Bt}} e^{\frac{x^2}{4D_n t}} dx = A \frac{\sqrt{D_n t 4\pi} H}{\sqrt{Bt}} \quad (21)$$

Where A is the section area of the semiconductor. By putting $B = D_n$ we get:

$$H = \frac{N}{A \sqrt{4\pi}} \quad (22)$$

We now obtain the solution by replacing H in the original equation:

$$n' = \frac{N}{A} \cdot \frac{1}{\sqrt{4\pi D_n t}} \cdot e^{-\frac{(x+\mu_n \varepsilon t)^2}{4D_n t} - \frac{t}{\tau_n}} \quad (23)$$

For the system at hand the generation due to the light source is $G = 2 \cdot 10^{22} \frac{1}{scm^3}$, the space interval Δx in which the generation takes place is $1\mu_m$ and the time interval is $\Delta t = 1 \cdot 10^{-12}s$, therefore:

$$G = 2 \cdot 10^{22} \frac{1}{scm^3} = 2 \cdot 10^{10} \frac{1}{s \mu_m^3} \quad (24)$$

$$\frac{N}{A} = G \cdot \Delta x \cdot \Delta t = 2 \cdot 10^{10} \cdot 10^{-12} = 2 \cdot 10^{-2} \frac{1}{(\mu_m)^2} \quad (25)$$

inserting this and the electric field for both cases in equation (23) gives the plots shown in figures 33 e 34.

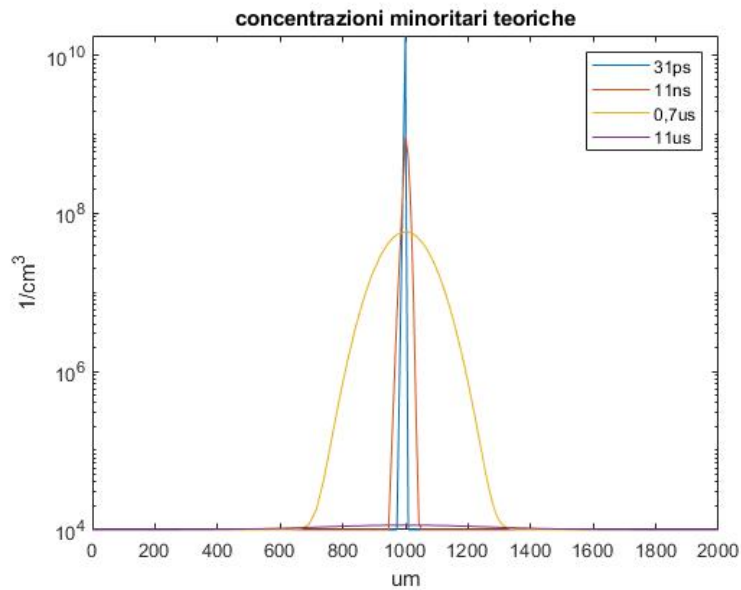


Figure 33: Electron concentration calculated for various time instants with electric field equal to zero

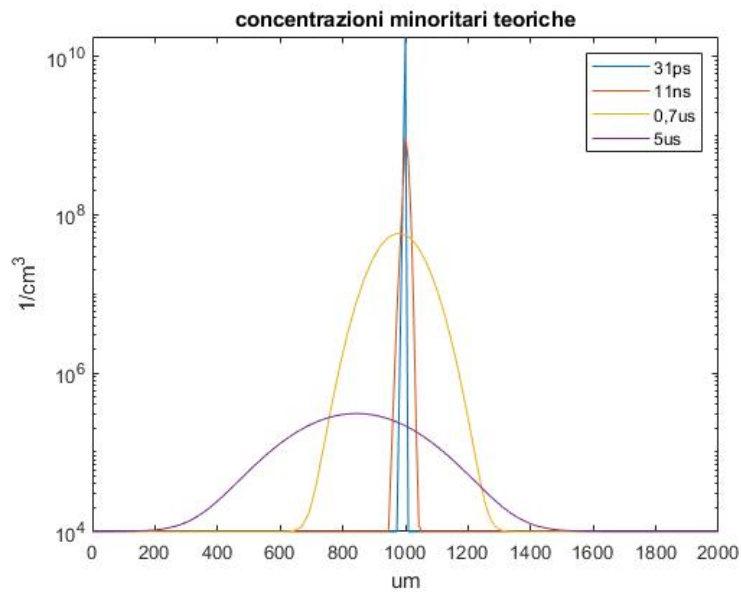


Figure 34: Electron concentration calculated for various time instants with non-zero electric field

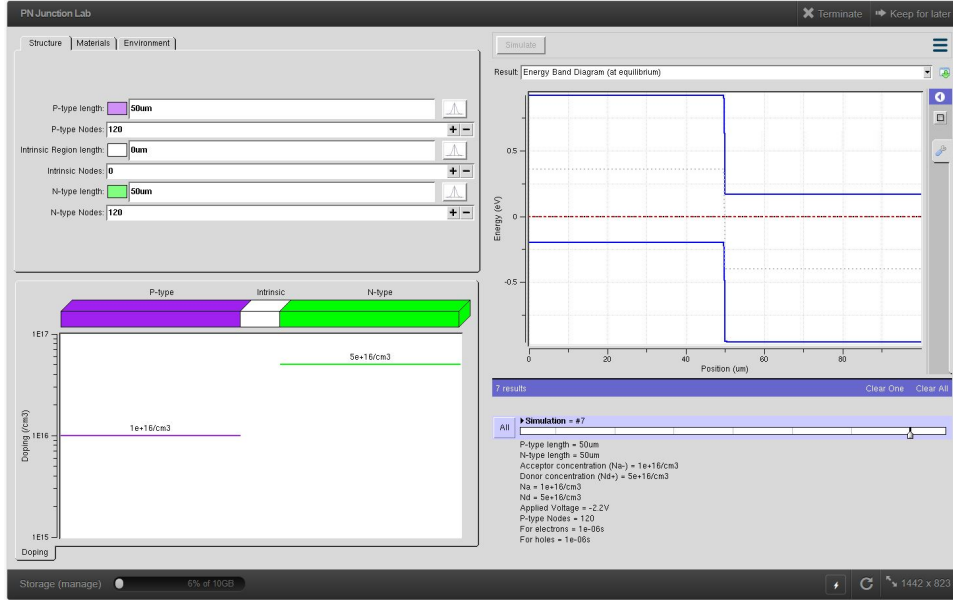


Figure 35: pn junction lab' user interface

3 PN junction

Let's move on to the analysis of a pn junction made of silicon and at room temperature. The doping levels of the two sides are $N_a = 10^{16} \text{ cm}^{-3}$ and $N_d = 5 \cdot 10^{16} \text{ cm}^{-3}$, the cross section is $A = 1 \text{ mm}^2$.

A very useful extension of Padre with a very clear user interface called 'pn junction lab' was used to simulate this system since it makes the whole process much easier.

3.1 Analysis

Once again we'll use Matlab to manipulate and study the results .

3.2 Band diagram, depletion region and electric field

Figure 36 clearly verifies our expectations, to check these results further we proceed to calculate the built in potential.

$$q\phi_{Sp} = q\chi + \frac{E_g}{2} + k_B T \ln\left(\frac{N_a}{n_i}\right) = 4.96 \text{ eV} \quad (26)$$

$$q\phi_{Sn} = q\chi + \frac{E_g}{2} + k_B T \ln\left(\frac{N_d}{n_i}\right) = 4.22 \text{ eV} \quad (27)$$

$$V_b i = q\phi_{Sp} - q\phi_{Sn} = 0.74 \text{ eV} \quad (28)$$

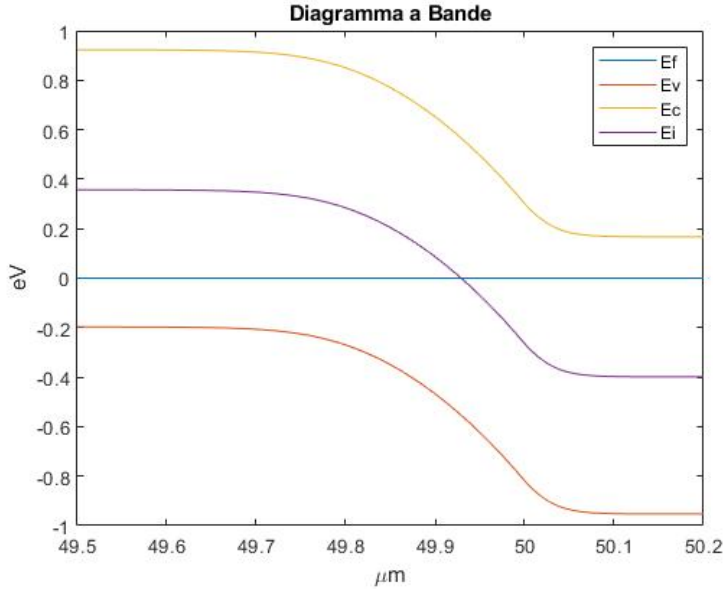


Figure 36: Simulated band diagram at equilibrium

Given the built in potential it's easy to find the depletion regions' dimensions:

$$x_{d0} = 339 \text{ nm} \quad (29)$$

$$x_{p0} = 282.5 \text{ nm} \quad (30)$$

$$x_{n0} = 56.5 \text{ nm} \quad (31)$$

Figure 37 shows a good match between theory and simulation for charge density.

The next step is to analyze the electric field:

$$\varepsilon(0) = -q \frac{N_a}{\epsilon} x_{p0} = -4.364 \cdot 10^4 \frac{V}{cm} \quad (32)$$

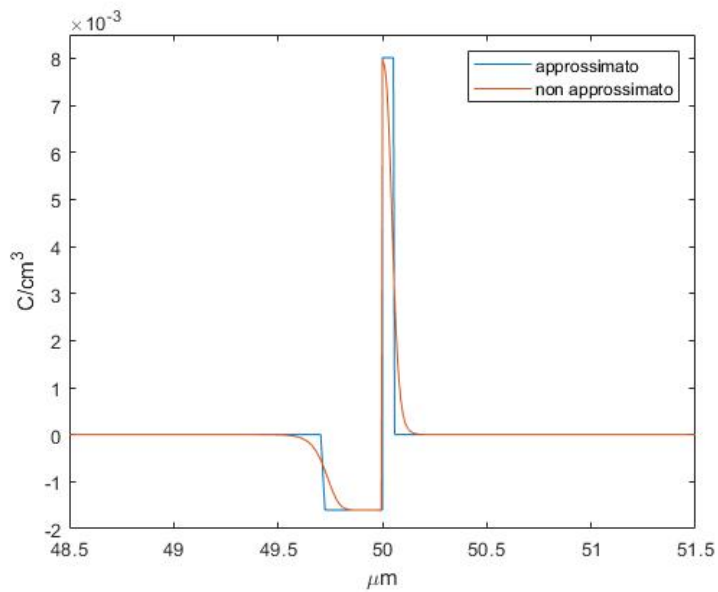


Figure 37: Charge density

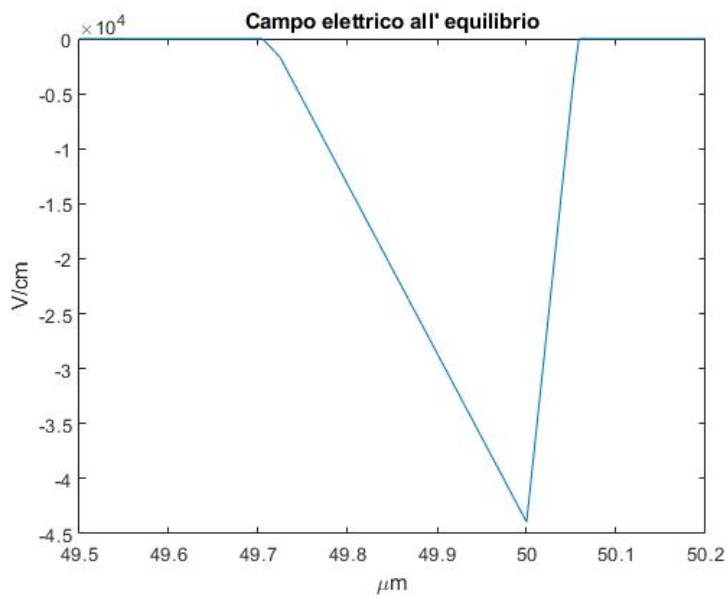


Figure 38: Electric field

```

log off

log acfile=plot31474-30.ac
  solve v1=0 vstep=-0.11578947368421054 nstep=20 elect=1
+      ac freq=10

log off

end

```

Figure 39: Capacitance effects code

3.3 Depletion region

Padre and all of its expansions (such as pn junction lab) allow us to see the capacitance effects acting in the system under examination, to be precise the code that makes it possible is shown in figure 39.

The command 'log' saves the simulation results that follow, we in fact close the previous log via 'log off' and proceed to open another one with 'log acfile=...'.

The Padre documentation tells us that a log command must follow this syntax:

Syntax

LOG file specification control

File specification can be either of these:

file specification

Outfile or Ivfile = filename

Acfile = filename

Acfile is used to save AC simulations data while outfile and ivfile are used for I-V profiles.

Right after these log lines there's a solve line that actually simulates the specified pn junction for various bias points.

This gives us a plot of the depletion capacitance per unit area as a function of voltage, shown in figure 40. The depletion capacitance is mathematically expressed as:

$$C_{dep} = A \sqrt{\frac{q\epsilon N_{eq}}{2(V_{bi} - V_a)}} \quad (33)$$

When $V_a = 0V$ we have

$$\text{Theoretical : } C_{dep}(0) = 305.6 \text{ pF} \quad (34)$$

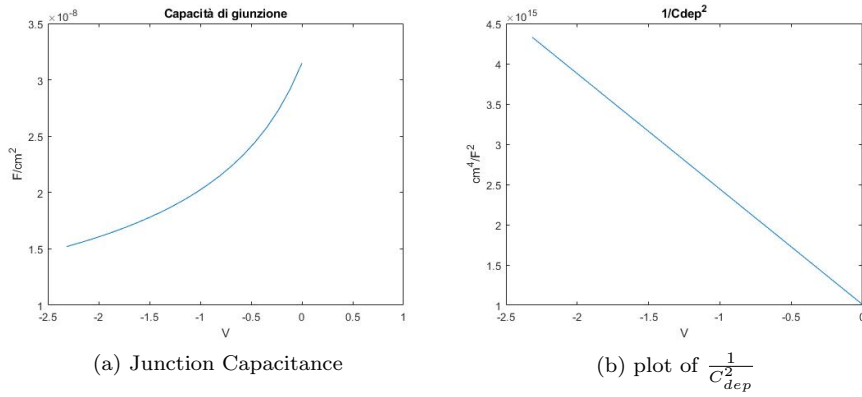


Figure 40: Junction Capacitance

$$\text{Simulated : } C_{dep}(0) = 314.8 \text{ pF} \quad (35)$$

We see a good match in this case as well which is even more convincing when seen graphically in figure 41.

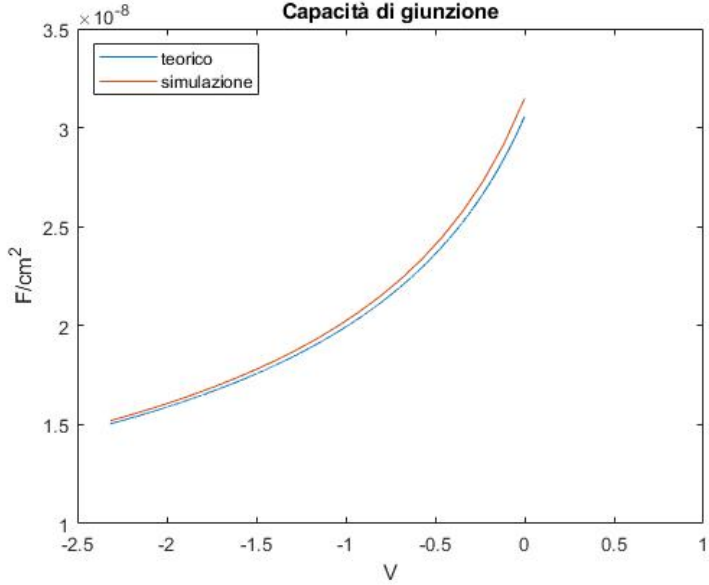


Figure 41: Junction capacitance comparison

3.4 Negative voltage

A slightly deeper look at the electric field lets us find the bias point V_a which doubles its value:

$$V_{bi} - V_a = -\frac{1}{2}x_d(V_a)\varepsilon(0)|_{V_a} \quad (36)$$

Knowing that,

$$x_d(V_a) = \sqrt{\frac{2\epsilon}{qN_{eq}}(V_{bi} - V_a)} \quad (37)$$

We can replace both $x_d(V_a)$ and $\varepsilon(0)|_{V_a}$ in equation (36),

$$V_{bi} - V_a = -\frac{1}{2}\sqrt{\frac{2\epsilon}{qN_{eq}}(V_{bi} - V_a) \cdot 2\varepsilon(0)|_{eq}} \quad (38)$$

Solving for V_a yields $V_a = -2.2V$.

A simple change in the bias settings in pn junction lab gives the simulated results which can be used to verify the previous calculations.

A negative voltage will result in some important changes such as an enlargement of the depletion region and of the voltage difference at the junction:

$$x_d(V_a) = \sqrt{\frac{2\epsilon}{qN_{eq}}(V_{bi} - V_a)} = 675.5\text{nm} \quad (39)$$

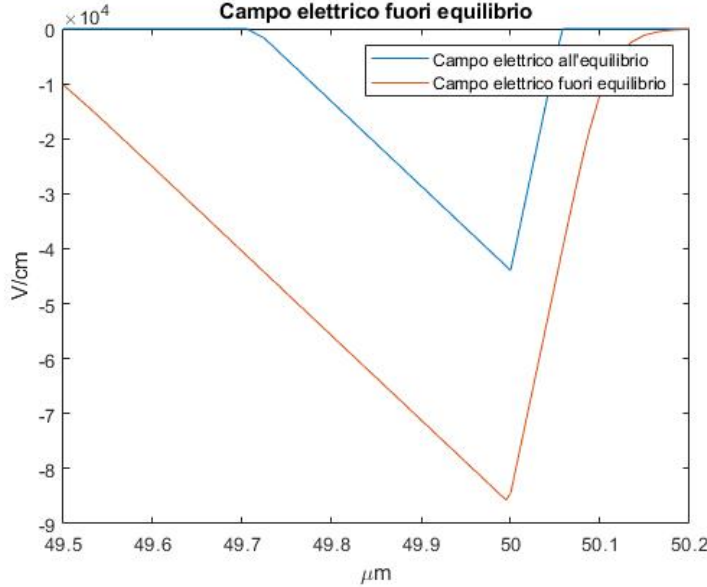


Figure 42: Electric field comparison for the two bias points

$$x_n = x_d \cdot \frac{N_a}{N_a + N_d} = 112.58 \text{ nm} \quad (40)$$

$$x_p = x_d \cdot \frac{N_d}{N_a + N_d} = 562.92 \text{ nm} \quad (41)$$

A quick glance at the band diagram confirms our predictions while creating some unsettling doubts concerning the Quasi Fermi levels which are assumed constant in the depletion region according to the theoretical model.

Using the n Quasi Fermi level as the 0eV value we get:

$$(E_{fn} - E_v)|_{+\infty} = -q\chi - E_g + q\phi_{sn} = -0.95 \text{ eV} \quad (42)$$

$$(E_{fp} - E_v)|_{+\infty} = q\chi + E_g - q\phi_{sp} = 0.21 \text{ eV} \quad (43)$$

Knowing the value of the voltage barrier and of the difference Efp-Ev we get Efp=2.2eV . Continuing to follow our theoretical model we expect these Quasi Fermi levels to drop off exponentially as the minority carriers go through the recombination process. The excess minority carriers' expression gives us an idea of this behaviour:

$$n'_p(x) = n'_p(-x_p) \frac{\sinh(\frac{w_p+x}{L_n})}{\sinh(\frac{w_p-x_p}{L_n})} \quad (44)$$

$$p'_n(x) = p'_n(x_n) \frac{\sinh(\frac{w_n-x}{L_p})}{\sinh(\frac{w_n-x_n}{L_p})} \quad (45)$$

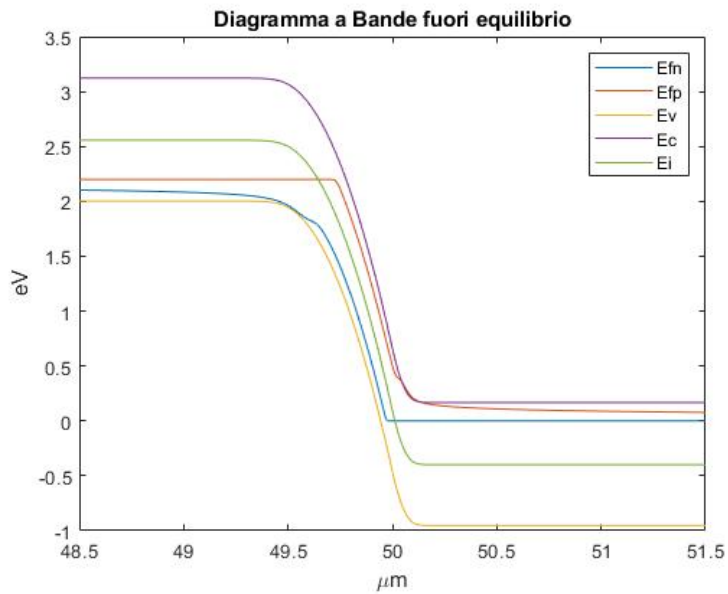


Figure 43: Band diagram for $V_a = -2.2V$

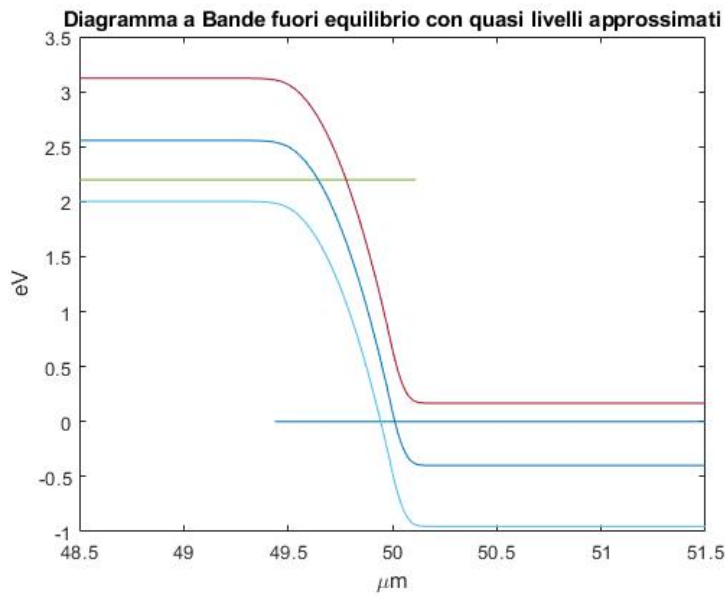


Figure 44: Theoretical band diagram

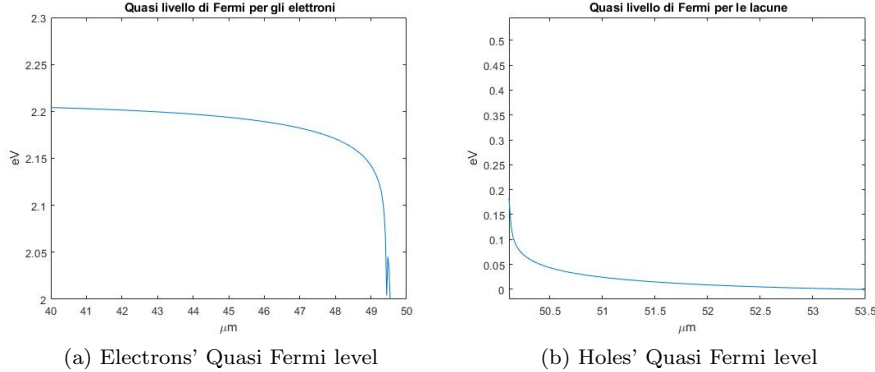


Figure 45: Quasi Fermi levels evolution

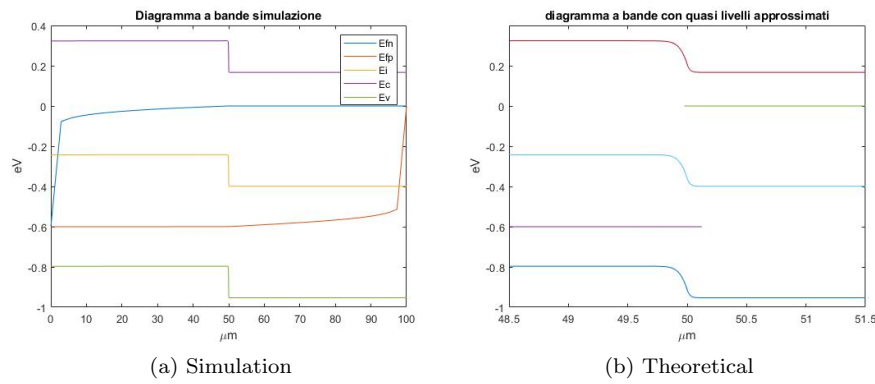


Figure 46: Band diagram comparison

$n'_p(-x_p)$ and $p'_n(x_n)$ where obtained through the junction laws.

Now the Shockley equations will lead us to the expressions of the Quasi Fermi levels:

$$E_{fn} = E_{fi} + KT \cdot \ln\left(\frac{n_{p0} + n'_p(x)}{n_i}\right) \quad (46)$$

$$E_{fp} = E_{fi} - KT \cdot \ln\left(\frac{p_{n0} + p'_n(x)}{n_i}\right) \quad (47)$$

Plugging these into Matlab yields figure 45.

3.5 Positive voltage

It's now interesting to see how this same examination plays out for a positive bias, such as $V_a=0.6V$. As we can see the Quasi Fermi levels are consistent

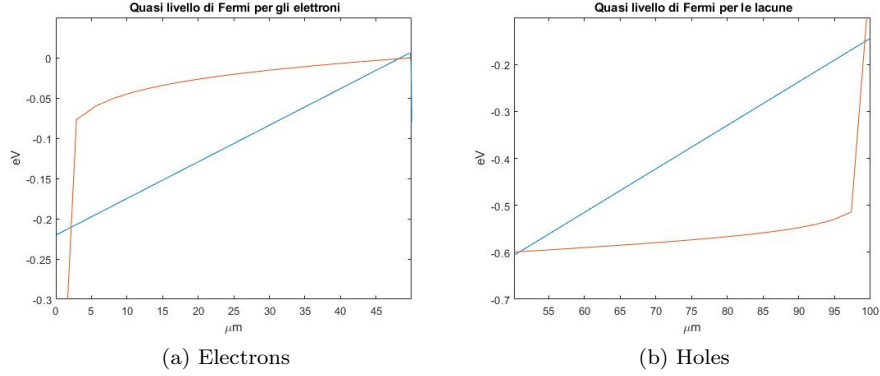


Figure 47: Evolution of Quasi Fermi levels (in red we see the simulated values and in blue the theoretical predictions)

between theory and simulation, at least in the zones in which they remain constant. The same calculations done before will give us the Quasi Fermi levels.

It must be emphasized that pn junction lab makes the contacts neutral by equating all the carrier concentrations to zero which justifies the graphs shown in figure 47. Another relevant observation is that we find many more minority carriers injected in this case rather than before:

$$n'_p(-x_p) = \frac{n_i^2}{N_a} \cdot (e^{\frac{V_a}{V_t}} - 1) = 2.21 \cdot 10^{14} \quad (48)$$

$$p'_n(x_n) = \frac{n_i^2}{N_d} \cdot (e^{\frac{V_a}{V_t}} - 1) = 4.42 \cdot 10^{13} \quad (49)$$

These values explain why the Quasi Fermi levels don't go back to their equilibrium value, all those carriers simply can't be recombined in just 50um.

3.6 Analysis of currents

We now move on to the calculation of the current generated by the minority carriers in the two neutral zones, the first step is finding the minority carriers (44) and (45). Figures 48 and 49 show the simulated values for minority carriers and their theoretical counterparts. There's clearly a problem which can once again be explained by looking at how Padre implements neutral contacts, it forces the concentrations to 0. This clearly changes the plot and the behaviour of our curves, the magnitude of the difference might not be apparent just by looking at the plots since the last value is in the order of 10^{12} , the raw data shown in figures 50 and 51 however makes it very clear.

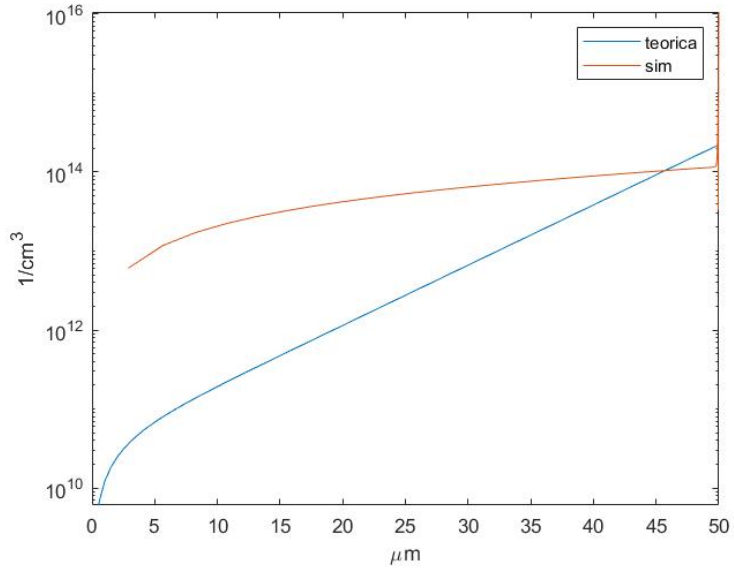


Figure 48: Electron concentration comparison

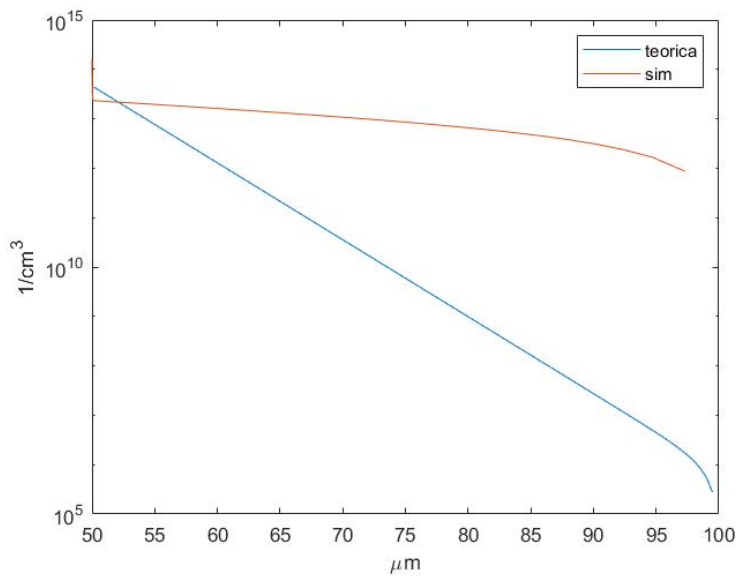


Figure 49: Holes concentration comparison

```

1  -----
2  n - Electron Density
3  -----
4  Position (um), Carrier Density (/cm3)
5      0,          0
6      2.89888737459,    6071887279084.62
7      5.65283038044,    11752948215874.6
8      8.26907623601,    17169090533374.6
9      10.7545097988,   22342949306474.6
10     13.1156716834,   27293528423274.6
11     15.3587754739,   32036888837474.6
12     17.4897240747,   36586684015274.6
13     19.5141252456,   40954596697574.6

```

Figure 50: raw data of the simulated electron concentration (μ_m on the left, cm^{-3} on the right)

475	70.2904990635,	10646749675414.9
476	72.5224891307,	9630022745144.92
477	74.9999981053,	8564902248054.92
478	76.5706333162,	7920400694374.92
479	78.2198002876,	7267409501164.92
480	79.9514256075,	6605771838124.92
481	81.7696321935,	5935095684054.92
482	83.6787491087,	5254687128134.92
483	85.6833218697,	4563468884144.92
484	87.7881232688,	3859879923794.92
485	89.9981647378,	3141749849114.92
486	92.3187082803,	2406135857104.92
487	94.7552789999,	1649088973794.92
488	97.3136782554,	865181106026.924
489	99.9999974738,	0

Figure 51: raw data of the simulated holes concentration (μ_m on the left, cm^{-3} on the right)

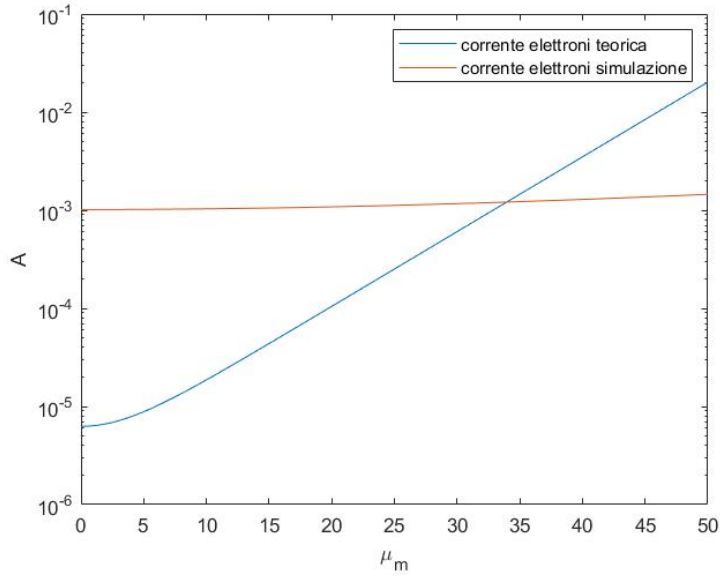


Figure 52: Electron current comparison

With this in mind we can proceed to compute the currents:

$$J_{n,diff}(x) = qAD_n \frac{dn'_p}{dx} = qA \frac{D_n}{L_n} n'_p(-x_p) \frac{\cosh(\frac{w_p+x}{L_n})}{\sinh(\frac{w_p-x_p}{L_n})} \quad (50)$$

$$J_{p,diff}(x) = -qAD_p \frac{dp'_n}{dx} = qA \frac{D_p}{L_p} p'_n(x_n) \frac{\cosh(\frac{w_n-x}{L_p})}{\sinh(\frac{w_n-x_n}{L_p})} \quad (51)$$

Just by looking at figures 52 and 53 it becomes apparent that the aforementioned error propagates throughout the simulation

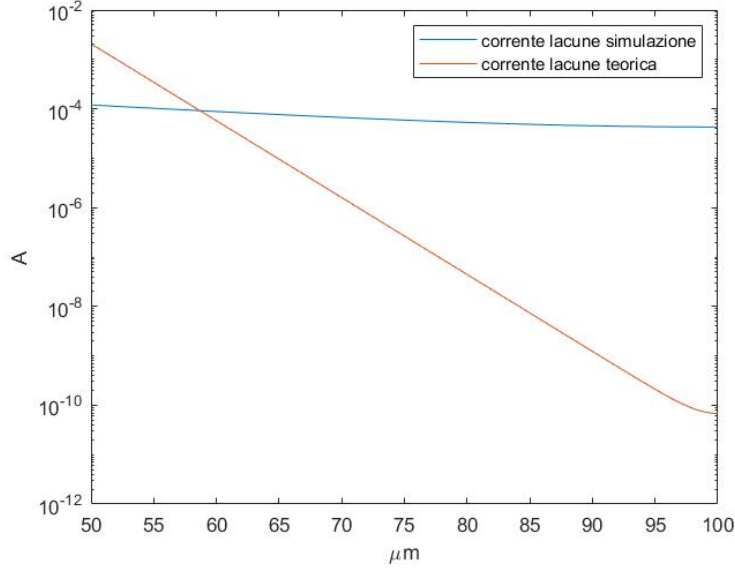


Figure 53: Hole current comparison

3.7 Generation-Recombination effects

While studying the currents in pn junctions, a very important equation pops up, the *ideal diode equation*:

$$J = J_s(e^{\frac{qV}{kT}} - 1) \quad (52)$$

J_s is

$$J_s = \frac{qD_p p_{n0}}{L_p} + \frac{qD_n n_{p0}}{L_n} \quad (53)$$

Using $\mu_n = 1250 \frac{cm^2}{Vs}$ and $\mu_p = 300 \frac{cm^2}{Vs}$ as parameters we get the behaviour shown in figure 54. We can use once again pn junction lab and Padre to compare theory and simulation (figures 55 and 56). It's clear that for low values of current the ideal model doesn't hold up. This is mainly due to the fact that in the depletion region some **generation and recombination processes** take place which aren't considered in the ideal diode equation.

Taking these effects into account complicates the mathematical expression:

$$J = \frac{qD_p p_{n0}}{L_p} e^{\frac{V}{V_t}} + \frac{qD_n n_{p0}}{L_n} e^{\frac{V}{V_t}} + q \frac{W}{2\tau_r} n_i e^{\frac{V}{2V_t}} \quad (54)$$

W is the depletion zone and τ_r is the recombination lifetime, calculated through the following equation:

$$\tau_r = \frac{1}{\sigma_0 v_{th} N_t} \quad (55)$$

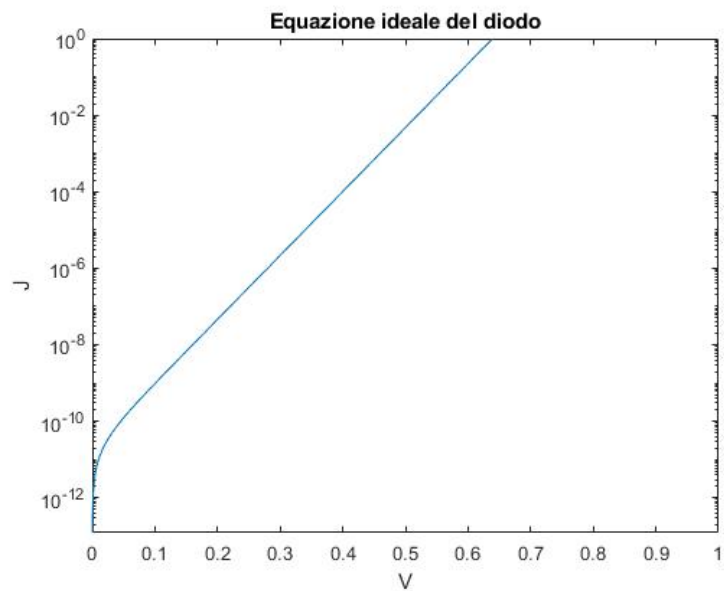


Figure 54: Ideal diode equation

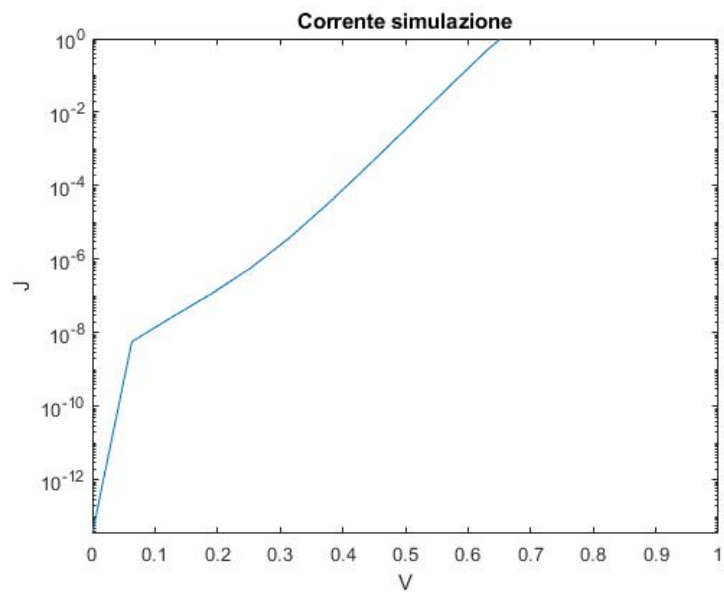


Figure 55: Simulated current

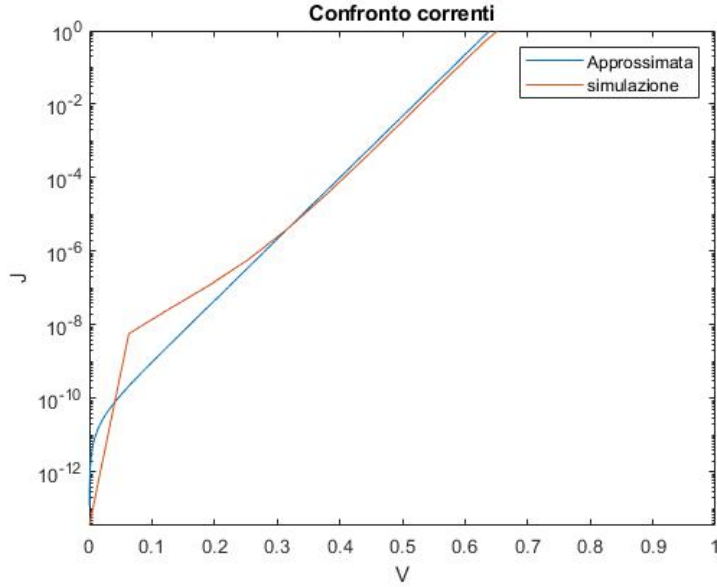


Figure 56: Simulation and ideal case comparison

These factors are,

- σ_0 is the recombination section which is a measure of the effectiveness of a recombination center in capturing an electron or a hole, its unit is cm^2 .
- v_{th} average thermal velocity , mathematically it's $v_{th}^2 = \frac{3KT}{m_n}$ where m_n is the effective mass of the electron.
- N_t recombination centers density , expressed in $\frac{atoms}{cm^2}$.

All these values are part of a particular recombination model known as Shockley-Read-Hall recombination. In order to proceed with our considerations we take reasonable values for σ_0 and N_t such as $10^{-15} cm^2$ and $10^{13} \frac{atoms}{cm^2}$ respectively.

Figure 57 lets us make some important observations, firstly we can see that this new expression approximates the simulation way more accurately than before.

Subsequently we can see that for low values of voltage and current the recombination current definitely prevails. This phenomenon can be analyzed further by taking the new expression for the current and introducing an *ideality factor* η . Let's rewrite the current in the following way:

$$J \propto e^{\frac{V}{\eta v_t}} \quad (56)$$

Taking $\eta \in [1, 2]$, some reasonable proportionality coefficients and plugging it all in Matlab gives figure 58. At first the graph closely follows that of $\eta = 2$

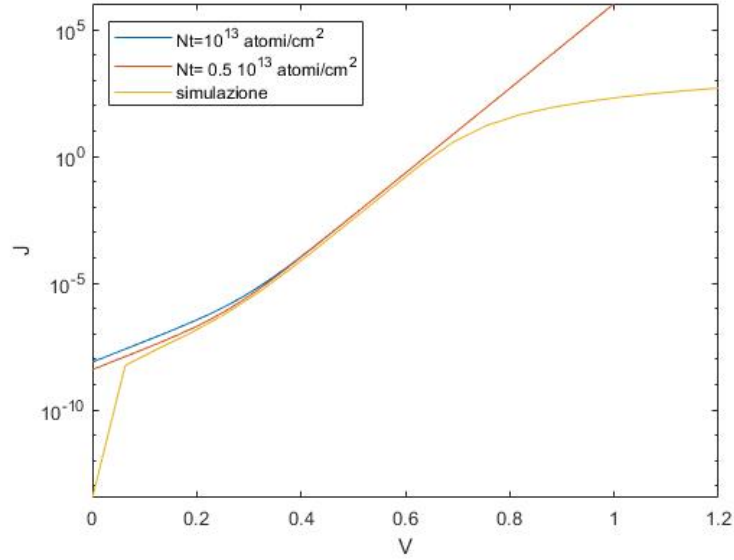


Figure 57: Currents comparison taking generation and recombination processes into account

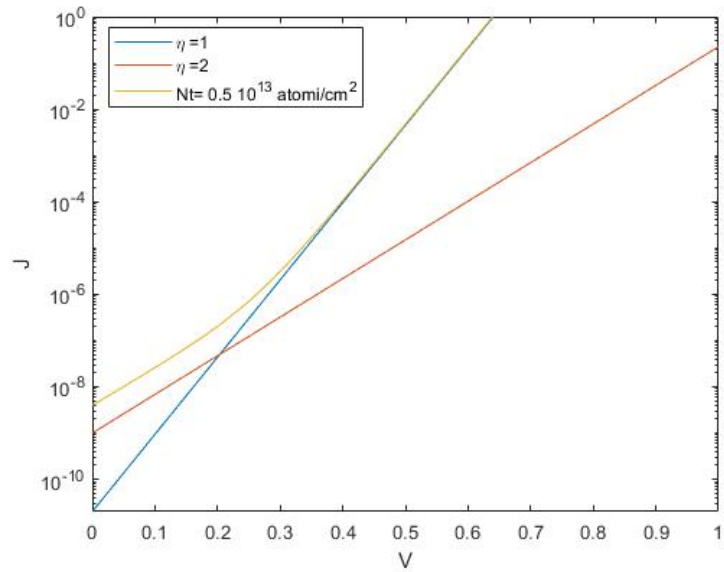


Figure 58: Comparison as η varies

(recombination current) only to later match the plot of $\eta = 1$.

However, there's a noticeable difference for greater values of voltage even taking recombination and generation processes into account.

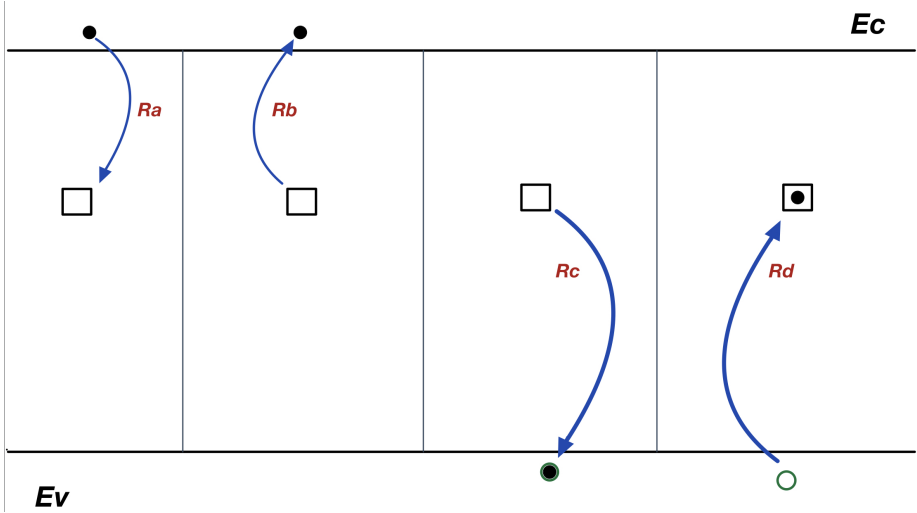


Figure 59: carriers-recombination centers interactions

4 SRH recombination model

The Shockley-Read-Hall (SRH) recombination model is a better approximation of the behaviour of some semiconductor devices rather than the simpler direct model.

The concept at the heart of this model is the interaction between carriers (electrons and holes) and the recombination centers which are localized in the forbidden band.

4.1 Fundamentals

Figure 59 shows a representation of the four main processes taking place in this new model:

- **R_a**, Capturing of an electron
- **R_b**, Emission of an electron
- **R_c**, Capturing of a hole
- **R_d**, Emission of an electron

Basically, there are some recombination centers at a given E_t in the forbidden band that facilitate the generation and recombination processes.

Supposing we call the density of recombination centers N_t and F the Fermi-Dirac function then the number of unoccupied states will be $N_t \cdot (1 - F)$:

$$F = \frac{1}{1 + e^{\frac{(E_t - E_f)}{kT}}} \quad (57)$$

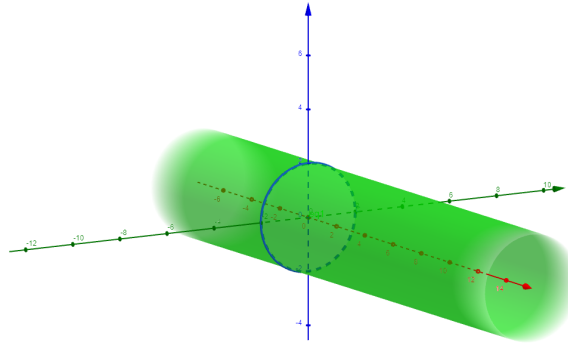


Figure 60: Visualization of the recombination section

We can intuitively guess that the capture speed of an electron is proportional to the total number of electrons and the number of unoccupied centers ($n \cdot N_t[1 - F]$). The full relation for Ra is:

$$Ra = v_{th} \sigma_n n N_t (1 - F) \quad (58)$$

v_{th} is the thermal velocity of carriers ($\frac{cm}{s}$) and σ_n is just the recombination section (cm^2).

In order to understand how $v_{th} \cdot \sigma_n$ is the correct proportionality constant it's helpful to look at figure 60.

Suppose an electron has a circular cross section (of area σ_n) just like the one shown in the plot and that this very electron moves along x with velocity v_{th} . It's easy to see that the volume occupied by the electron as time passes is a cylinder (dimensionally $v_{th} \cdot \sigma_n$ is $\frac{cm^3}{s}$) and **if the recombination center happens to be in that cylinder then the electron gets captured**.

At this point it would be interesting to see how the capturing rate changes as Et, the recombination centers' energy level, varies. Let's analyze a simple slab of semiconductor p doped $N_a = 10^{17}$ and take the following values:

- $\sigma_0 = 5 \cdot 10^{-15} cm^2$
- $N_t = 2 \cdot 10^{15} \frac{atoms}{cm^3}$
- $v_{th} = 10^7 \frac{cm}{s}$
- $n = 2102.5 \frac{1}{cm^3}$

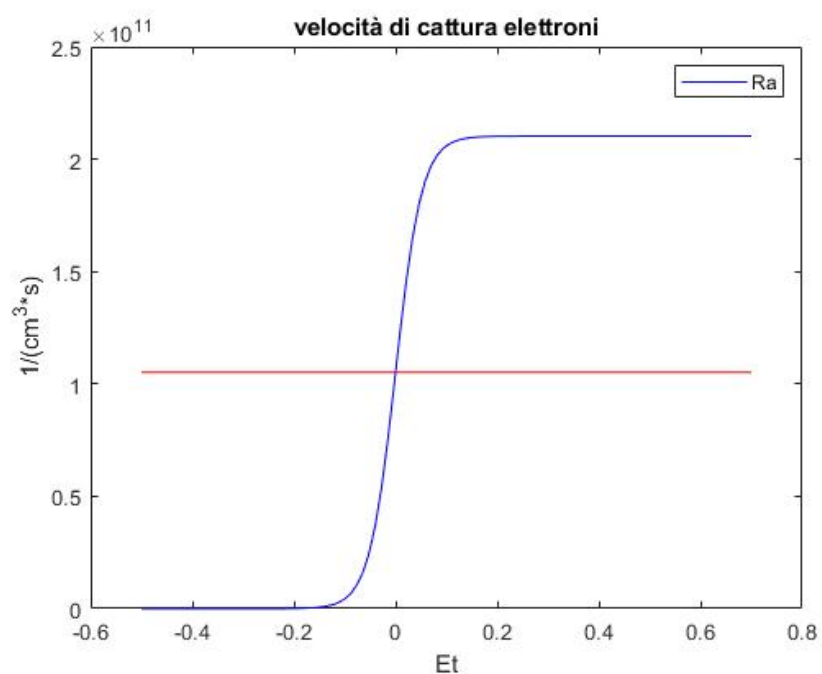


Figure 61: Ra

Figure 61 shows the capturing rate in blue and in red its value when E_t equals the Fermi level.

As E_t increases so does R_a , this is physically justifiable simply by imagining that for high energy levels the probability of them being occupied decreases and the recombination centers will therefore be available to capture electrons.

In order to balance this phenomenon we also have the emission of electrons which is shown in the second part of figure 1. In this case the expression will be proportional to the number of free unoccupied recombination centers:

$$R_b = e_n \cdot N_t F \quad (59)$$

We can find the proportionality constant called *emission probability* simply by saying that at equilibrium these two processes must be equal. :

$$Ra = Rb \quad (60)$$

$$v_{th} \sigma_n n N_t (1 - F) = e_n \cdot N_t F \quad (61)$$

$$e_n = \frac{v_{th} \sigma_n n (1 - F)}{F} \quad (62)$$

Howeverwe can see that:

$$\frac{1 - F}{F} = \frac{1 - \frac{1}{1 + e^{\frac{E_t - E_f}{KT}}}}{\frac{1}{1 + e^{\frac{E_t - E_f}{KT}}}} = \frac{1}{\frac{1}{1 + e^{\frac{E_t - E_f}{KT}}}} - 1 = e^{\frac{E_t - E_f}{KT}} \quad (63)$$

and according to Shockley,

$$n = n_i \cdot e^{\frac{E_f - E_i}{KT}} \quad (64)$$

Replacing (63) and (64) in equation (62) yields:

$$e_n = v_{th} \sigma_n n_i \cdot e^{\frac{E_t - E_i}{KT}} \quad (65)$$

Figure 62 shows exactly what we predicted, as the energy level increase the probability of an electron passing into the conduction band decreases.

We can proceed in the exact same manner for R_c and R_d .

$$R_c = v_{th} \sigma_p p N_t F \quad (66)$$

$$R_d = e_p \cdot N_t (1 - F) \quad (67)$$

$$e_p = v_{th} \sigma_p n_i \cdot e^{\frac{E_i - E_t}{KT}} \quad (68)$$

Figures 63 and 64 show a total symmetry in these processes.

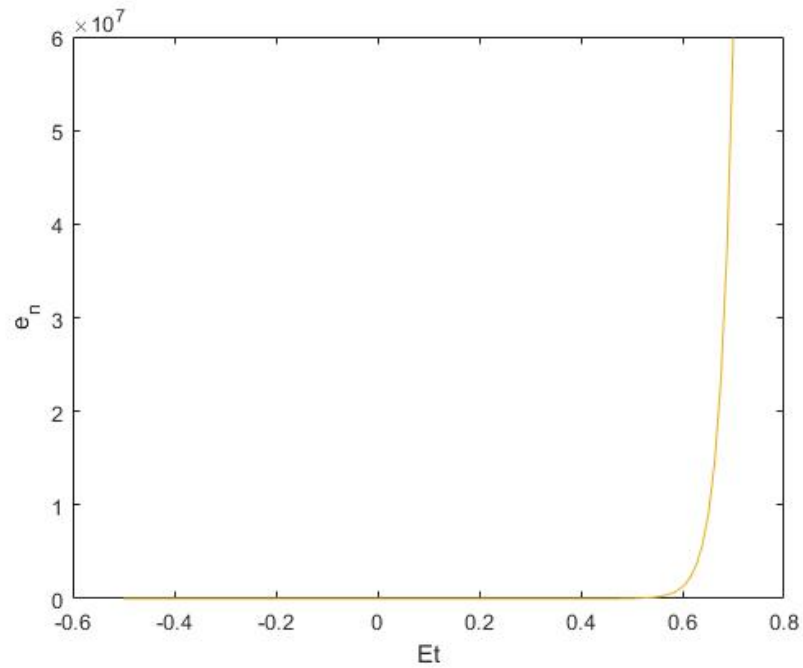


Figure 62: Electron emission probability

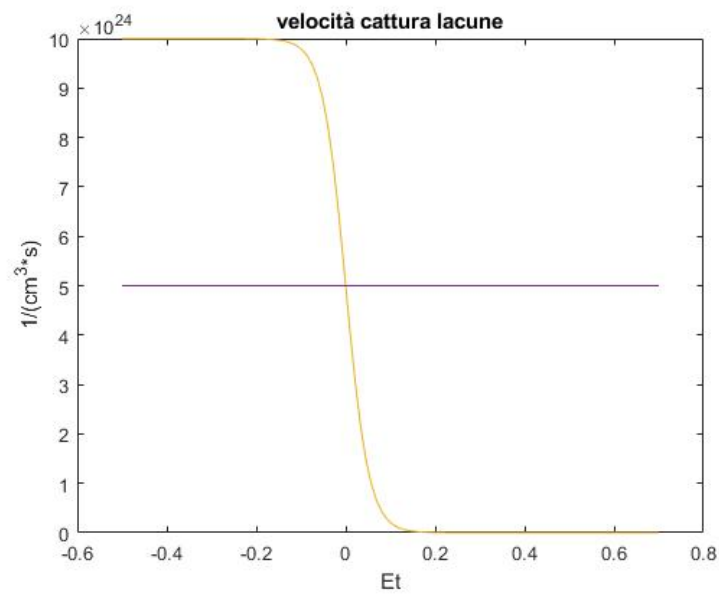


Figure 63: Holes capturing rate

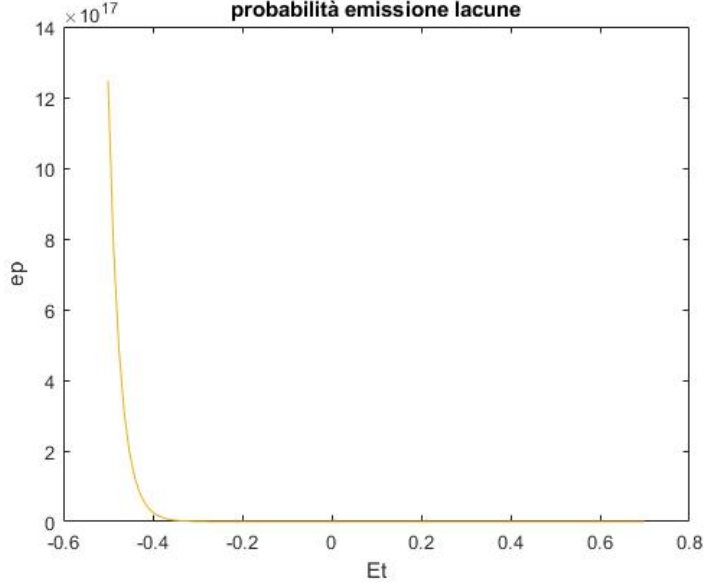


Figure 64: Holes emission probability

4.2 Recombination rate

In order to find the recombination rate U we notice that the principle of **charge conservation** holds true even out of equilibrium:

$$Ra - Rb = Rc - Rd \quad (69)$$

We can proceed by replacing the relations obtained before into equation (69):

$$v_{th}\sigma_n N_t [n(1-F) - F \cdot n_i \cdot e^{\frac{E_i - E_t}{KT}}] = v_{th}\sigma_p N_t [p \cdot F - n_i \cdot e^{\frac{E_i - E_t}{KT}} + n_i \cdot e^{\frac{E_i - E_t}{KT}} F] \quad (70)$$

It's crucial to observe that we are finding a general equation that is true even out of equilibrium, therefore we can no longer consider F as a known quantity and we'll need to explicitly find it.

$$v_{th}\sigma_n N_t n + v_{th}\sigma_p N_t n_i \cdot e^{\frac{E_i - E_t}{KT}} = F \cdot v_{th} N_t (\sigma_p p + \sigma_p n_i e^{\frac{E_i - E_t}{KT}} + \sigma_n n + \sigma_n n_i e^{\frac{E_t - E_i}{KT}}) \quad (71)$$

$$F = \frac{v_{th}\sigma_n N_t n + v_{th}\sigma_p N_t n_i \cdot e^{\frac{E_i - E_t}{KT}}}{v_{th} N_t (\sigma_p p + \sigma_p n_i e^{\frac{E_i - E_t}{KT}} + \sigma_n n + \sigma_n n_i e^{\frac{E_t - E_i}{KT}})} \quad (72)$$

F is:

$$F = \frac{\sigma_n n + \sigma_p n_i e^{\frac{E_i - E_t}{KT}}}{\sigma_p p + \sigma_p n_i e^{\frac{E_i - E_t}{KT}} + \sigma_n n + \sigma_n n_i e^{\frac{E_t - E_i}{KT}}} \quad (73)$$

Replacing this in the left hand side of (70) gives us \mathbf{U} independently of F:

$$Ra - Rb = \mathbf{U} = v_{th}\sigma_n N_t \cdot \frac{\sigma_p(pn - n_i^2)}{\sigma_p(p + n_i e^{\frac{Ei-Et}{KT}}) + \sigma_n(n + n_i e^{\frac{Et-Ei}{KT}})} \quad (74)$$

4.3 Padre comparison

4.4 Theoretical analysis

The simulated system is a simple slab of semiconductor with length $L = 400\mu_m$ and p doping $Na = 10^{17}\frac{1}{cm^3}$, no bias is applied but there's a light source shining on the left side of the semiconductor with generation rate $2 \cdot 10^{20}\frac{1}{cm^3.s}$.

We will primarily analyze the evolution of minority carriers and what their dependence is with respects to the energy level Et. In order to do this the mathematical expression for \mathbf{U} must be simplified.

Firstly we can suppose that the recombination section of holes and electrons are the same $\sigma_p = \sigma_n = \sigma_0$:

$$\mathbf{U} = v_{th}\sigma_0 N_t \cdot \frac{(pn - n_i^2)}{p + n + 2n_i \cosh(\frac{Et-Ei}{KT})} \quad (75)$$

We can also assume that we are in a *low injection level* regime which leads to the following simplification:

$$\mathbf{U} = v_{th}\sigma_0 N_t \cdot \frac{(n - n_0)}{1 + \frac{2n_i}{n_0 + p_0} \cosh(\frac{Et-Ei}{KT})} \quad (76)$$

We define τ_r as follows:

$$\tau_r \equiv \frac{1 + \frac{2n_i}{n_0 + p_0} \cosh(\frac{Et-Ei}{KT})}{v_{th}\sigma_0 N_t} \quad (77)$$

So \mathbf{U} can now be rewritten as:

$$\mathbf{U} = \frac{n - n_0}{\tau_r} \quad (78)$$

Now we move on to the minority carriers concentration:

$$\frac{dn}{dt} = \frac{1}{q} \cdot \frac{dJ_n}{dx} - \mathbf{U} \quad (79)$$

e

$$J_n = qn\mu_n\varepsilon + qD_n \frac{dn}{dx} \quad (80)$$

In this particular situation the electric field ε should be 0 since there's no voltage applied, this very condition paired with the stationarity ($\frac{dn}{dt} = 0$) transforms equation (80) into:

$$D_n \frac{d^2n}{dx^2} - \mathbf{U} = D_n \frac{d^2n}{dx^2} - \frac{n'}{\tau_r} = 0 \quad (81)$$

```

ETrap      = vector      trap energy levels = Et - Ei (eV)
NTRap     = vector      trap densities (/cm**3)

```

Figure 65: Padre manual

The characteristic equation then becomes:

$$D_n \cdot \lambda^2 - \frac{1}{\tau_r} = 0 \quad (82)$$

Its roots are:

$$\lambda_{1,2} = \pm \frac{1}{\sqrt{D_n \tau_r}} \quad (83)$$

The general solution is:

$$n'(x) = A \cdot e^{\frac{x}{\sqrt{D_n \tau_r}}} + B \cdot e^{-\frac{x}{\sqrt{D_n \tau_r}}} \quad (84)$$

We know that the length L is much bigger than the diffusion length of the carriers which leads to A=0, in addition to this we also know n'(0):

$$n'(x) = n'(0) \cdot e^{-\frac{x}{\sqrt{D_n \tau_r}}} \quad (85)$$

4.5 Simulation

Padre only allows us **to manipulate two parameters** of the model just described: Nt e $Et - Ei$ (figure 65). In order to have congruence between simulation and theory, in Padre we choose a value for the electron lifetime $10^{-6}s$ (Padre command: taun0=1e-6), this means that (for $Et=Ei$):

$$\tau_r = \frac{1}{v_{th} \sigma_0 N_t} = 10^{-6}s \quad (86)$$

We force the mobility to $\mu_n = 1247 \frac{cm^2}{s}$ and for $n'(0)$ we'll use the value given by Padre, replacing in (85) gives us figure 66. Now we change the position (energetically) of the recombination centers simply by writing "etrap=0.4" in the Material line, this means that $Et-Ei=0.4$ and that the hyperbolic cosine in τ_r is no longer equal to 1. This forces use to use expression (77) instead of (86) giving figure 67.

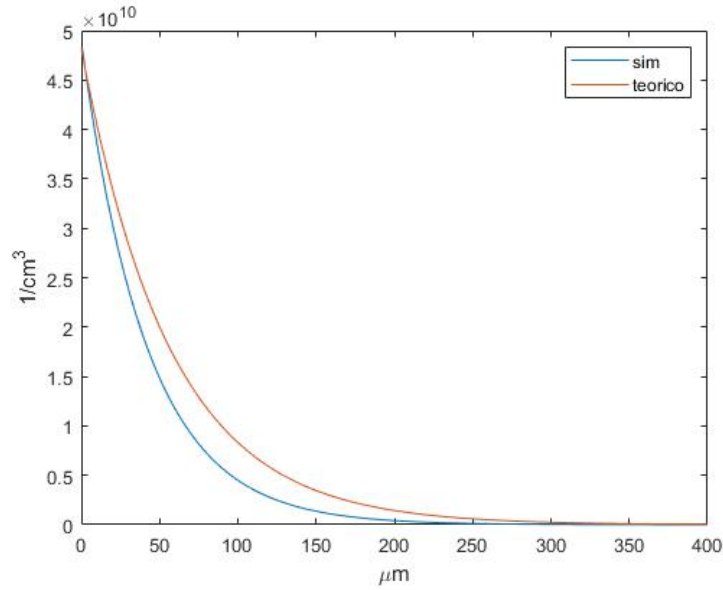


Figure 66: Minority carriers with $E_t = E_i$

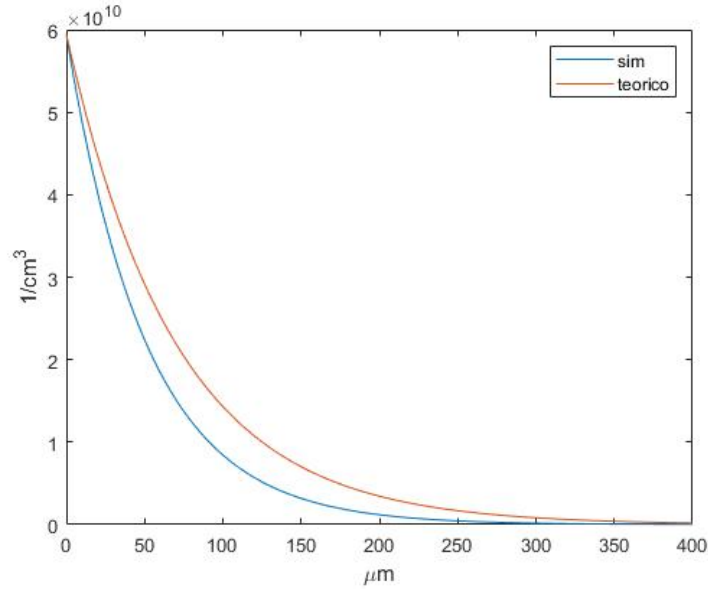


Figure 67: Minority carriers with $E_t - E_i = 0,4$

Boundary Value Problems

R2021a

Boundary value problem solvers for ordinary differential equations

Boundary value problems (BVPs) are ordinary differential equations that are subject to boundary conditions. Unlike initial value problems, a BVP can have a finite solution, no solution, or infinitely many solutions. The initial guess of the solution is an integral part of solving a BVP, and the quality of the guess can be critical for the solver performance or even for a successful computation. The `bvp4c` and `bvp5c` solvers work on boundary value problems that have two-point boundary conditions, multipoint conditions, singularities in the solutions, or unknown parameters. For more information, see [Solving Boundary Value Problems](#).

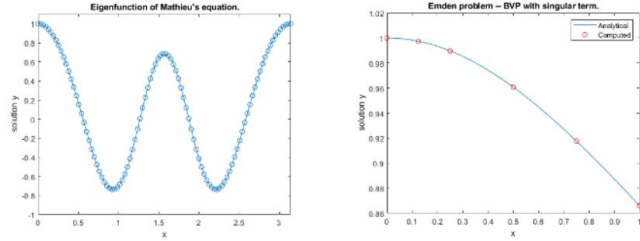


Figure 68: bvp5c description

It's clear that the model we used is a gross approximation of the simulated case. To fix this some approximations must be taken out in the method used to get to (85), the most obvious is the one concerning the recombination section:

$$\sigma_p = \sigma_n = \sigma_0 \quad (87)$$

Removing this leads us back to (74) which means that now the differential equation is:

$$D_n \frac{d^2 n}{dx^2} - \mathbf{U} = D_n \frac{d^2 n}{dx^2} - v_{th} \sigma_n N_t \cdot \frac{\sigma_p (pn - n_i^2)}{\sigma_p (p + n_i e^{\frac{E_i - E_t}{KT}}) + \sigma_n (n + n_i e^{\frac{E_t - E_i}{KT}})} = 0 \quad (88)$$

To solve this we use a Matlab command called `bvp5c`. This brief description underlines the importance the "**initial guess**" has in the solution. In our case, unless we solve the differential equation analytically, we are forced to use the expression of figures 66 and 67 as initial guesses. Three files were created for each situation in Matlab ($E_t - E_i = 0$, $E_t - E_i = 0.4$):

- **eqne.m**, here the equation is described (figure 69), it's crucial to see that (88) was disassembled into a system of first order differential equations in line 9.
- **bfcfn.m**, here the boundary conditions are specified, each element of the res vector in line 2 is equated to 0, for example the first element is $n'(0) = 4.818e10$ (figure 70).
- **guess.m**, this function implements the prediction described above. In order to understand figure 71 it's important to remember that the original differential equation was broken in two parts:

Equation 1

$$\frac{dn_1}{dx} = n_2 \quad (89)$$

```

1  function equazione=eqne (x,n)
2 -   Dn=3.242e9;
3 -   vth=1e7;
4 -   sigman=1.8e-16;
5 -   sigmap=1e-15;
6 -   Nt=1e15;
7 -   p=1e17;
8 -   ni=9.96262e9;
9 -   equazione=[n(2); (Nt*sigman*sigmap*vth*(p*n(1)-ni^2)/(Dn*(p+ni)*sigmap+sigman*(n(1)+ni))];

```

Figure 69: eqne.m

```

1  function res=bfcfn(na,nb)
2 -   res=[na(1)-4.818e10  nb(1)];
3 -   end

```

Figure 70: bfcfn.m

Equation 2

$$\frac{dn_2}{dx} = v_{th} \sigma_n N_t \cdot \frac{\sigma_p (pn_1 - n_i^2)}{D_n (\sigma_p (p + n_i e^{\frac{E_i - Et}{KT}}) + \sigma_n (n_1 + n_i e^{\frac{Et - E_i}{KT}}))} \quad (90)$$

All the functions described above are put together through the code shown in figure 72, by executing that code and choosing $\sigma_{n,i}$ in eqne.m as to have perfect congruence we arrive at figure 73.

```

1  function g=guess(x)
2 -   g=[ (sqrt(3.242e9*1e-6).*exp(x./sqrt(3.242e9*1e-6)))  exp(x./sqrt(3.242e9*1e-6))];
3 -   end

```

Figure 71: guess.m

```

2451 -      xmesh=linspace(0,400,237);
2452 -      solinit=bvpinit(xmesh,@guess);
2453
2454 -      sol=bvp5c(@eqne,@bcfcn,solinit)
2455
2456
2457
2458 -      figure(16);
2459 -      plot(xn,n0);
2460 -      hold on;
2461 -      plot(sol.x,sol.y(1,:));
2462 -      legend('simulazione','soluzione numerica');
2463 -      hold off;

```

Figure 72: bvp5c usage

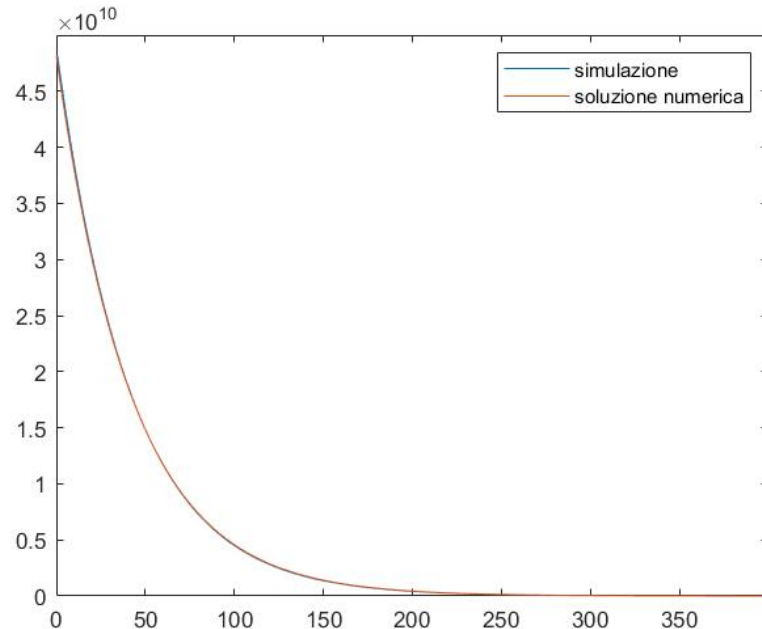


Figure 73: Comparison between simulation and bvp5c result

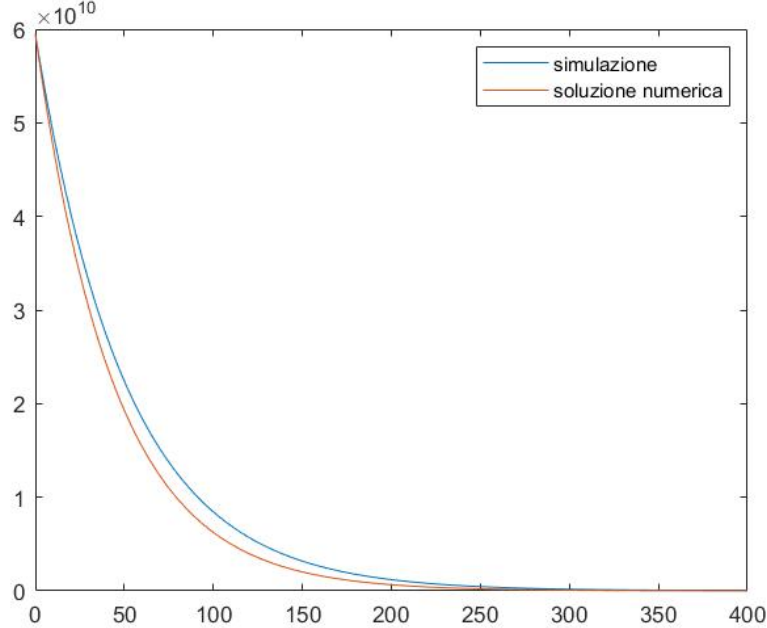


Figure 74: Comparison between simulation and bvp5c result, Et-Ei=0.4

It's important to notice that the matching of the curve comes from a supposition regarding σ_n . We don't know what values of σ_n and σ_p are used by Padre so the best we can do is make sure that all the others parameters coincide (v_{th}, D_n, N_t, p e n_i) and impose $\sigma_n = 1.8 \cdot 10^{-16}$ afterwards in order to have congruence. Even though the congruence is somewhat artificial it's still relevant to notice that the numerical solution found by Matlab is of the correct form . Repeating this procedure with the new σ_n gives the behaviour of minority carriers for Et-Ei=0.4, shown in comparison with the simulation in figure 74.

Figure 74 shows a great improvement from the previous case with the simplified model. It also shows a slight difference in the curves that might be due to a bad guess in the file guess.m. In fact it must be noted that since we haven't analytically solved the differential equation the curve used as prediction is the one shown in figure 67 which, as stated before, is a gross approximation of the simulation.

References

- [1] Mark R. Pinto, kent smith, Muhammad Alam, Steven Clark, Xufeng Wang, Gerhard Klimeck, Dragica Vasileska (2014), "Padre,"

<https://nanohub.org/resources/padre>. (DOI: 10.4231/D30C4SK7Z).
Manuale Padre.

- [2] Saumitra Raj Mehrotra, Abhijeet Paul, Gerhard Klimeck, Gloria Wahyu Budiman (2014), "Drift-Diffusion Lab," <https://nanohub.org/resources/semi>. (DOI: 10.4231/D3M90239B).
Drift Diffusion Lab
- [3] Dragica Vasileska, Matteo Mannino, Michael McLennan, Xufeng Wang, Gerhard Klimeck, Saumitra Raj Mehrotra, Benjamin P Haley (2014), "PN Junction Lab," <https://nanohub.org/resources/pntoy>. (DOI: 10.4231/D3GH9B95N).
PN Junction Lab